A PRACTICAL APPROACH FOR ULTRA HIGH PERFORMANCE CONCRETE CONSTRUCTION

By

Yang Chen

A THESIS

Submitted to
Michigan State University
in partial fulfillment of the requirements
for the degree of

Civil Engineering—Master of Science

2017

ABSTRACT

A PRACTICAL APPROACH FOR ULTRA HIGH PERFORMANCE CONCRETE CONSTRUCTION

By

Yang Chen

Ultra-high-performance concrete (UHPC) with compressive strengths in excess of 150 MPa promise to enhance the structural efficiency and durability of concrete-based infrastructure systems. In order to transition UHPC materials into mainstream construction practices, there are needs to develop refined mix design procedures that enable production of UHPC using primarily locally available materials, resolves the problems with production of homogeneous UHPC mixtures using commonly available concrete mixers, develop convenient fresh mix workability test methods that consider the peculiar rheology of fresh UHPC mixtures, and quantify some aspects of the UHPC material properties that have not been fully characterized.

The UHPC materials were tested for fresh mix flow and hardened concrete compressive strength. The trends in the effects of packing density, water film thickness and excess paste film thickness on compressive strength and fresh mix flow were investigated. The results were used to identify viable ranges of these defining characteristics of UHPC mixtures. Response surface analysis of the fresh mix flow and the hardened concrete compressive strength test results led to identification of the optimum values of mix design parameters. The optimum mix was prepared, and was found to produce a highly desired balance of fresh mix flow and hardened concrete compressive strength, which occurred within the ranges predicted by response surface analysis of experimental results.

TABLE OF CONTENTS

LIST OF TABLES

LIST OF FIGURES

INTRODUCTION

Background

Ultra-high-performance concrete is a relatively new class of advanced cementitious materials, with compressive strength and tensile strength exceeding 150MPa and 7 MPa, respectively. UHPC mixtures are generally designed with relatively high dosages of silica fume, superplasticizer and steel fiber, rand relatively small aggregate contents. Conventional concrete mix design procedures cannot be applied to UHPC mixtures. There are also challenges relating to production, and the fresh mix rheology, surface quality and dimensional stability of UHPC. This M.S. dissertation research was conducted to address these issues in an effort to facilitate design, production and quality control of UHPC in mainstream construction applications.

Objective and Scope

- Develop refined mix designs to enable production of UHPC using primarily locally available materials.
- Tailor the fiber reinforcement conditions of UHPC to enable production with commonly available (rotary drum) concrete mixers without encountering the fiber balling problem.
- Thoroughly assess the fresh mix rheology of UHPC, and devise convenient and rapid field test methods for evaluation of the fresh UHPC mix rheology to resolve the variabilities associated with the lack of control over the water content of UHPC in industrial-scale production facilities.
- Resolve the surface quality challenges encountered in large-scale construction with UHPC.
- Characterize the dimensional stability aspects of the UHPC performance, which are affected by its high contents of cementitious materials and low water content.

Organization of Content

This thesis is organized into four chapters. Development of refined mix design procedures is presented in the first chapter. The second chapter covers the efforts devoted in this research to resolving the fiber dispersion problem encountered when UHPC is produced in commonly available rotary drum mixers, thoroughly evaluating the fresh UHPC mix rheology, and developing convenient and rapid test methods for field evaluation of the UHPC rheology for adjusting its water content. The focus of the third chapter is on improving the surface quality of UHPC, which tends to be compromised by loss of its low water content to near-surface evaporation, which cannot be replaced by bleeding. The fourth chapter of the thesis covers the experimental investigations conducted in order to gain insight into the dimensional stability of UHPC that are affected by its high contents and complex nature of cementitious materials, and its distinctly low water content.

CHAPTER 1

Optimization of Ultra-High Performance Concrete, Quantification of Characteristic Features

Abstract

An optimization experimental program was designed based on response surface principles in order to identify a desired balance of some key mix design parameters for ultra-high-performance concrete (UHPC). The following mix design parameters were evaluated: superplasticizer content, coarse-to-fine aggregate ratio, and fiber volume fraction. The values of packing density, water film thickness and excess paste film thickness were calculated for the UHPC mix designs which were subject of this optimization experimental program. The UHPC materials were tested for fresh mix flow and hardened concrete compressive strength. The trends in the effects of packing density, water film thickness and excess paste film thickness on compressive strength and fresh mix flow were investigated. The results were used to identify viable ranges of these defining characteristics of UHPC mixtures. Response surface analysis of the fresh mix flow and the hardened concrete compressive strength test results led to identification of the optimum values of mix design parameters. The optimum mix was prepared, and was found to produce a highly desired balance of fresh mix flow and hardened concrete compressive strength, which occurred within the ranges predicted by response surface analysis of experimental results. The calculated values of packing density, water film thickness and excess paste film thickness were also within the viable ranges identified in the project.

Introduction

Ultra-high-performance concrete (UHPC) is a relatively new class of advanced cementitious materials, which provide compressive and tensile strengths exceeding 150 MPa and 7 MPa, respectively (Aïtcin, 2011). UHPC mixtures are generally designed with relatively high dosages

of silica fume, superplasticizer and steel fiber, relatively small concentrations of aggregates of relatively small size, and Portland cement and typically another pozzolan (e.g., fly ash or silica fume) (Peyvandi et al.). Some distinguishing features of UHPC include an optimized gradation of the granular matter for realizing high packing densities, water-to-cementitious materials ratios of less than 0.25, and a relatively high volume fraction of discrete (steel) fibers (Schießl et al., 2007). Examples of UHPC application include a pedestrian bridge at Sherbrooke (Canada) constructed in 1997, replacement of the steel parts of a cooling tower at Cattenom, and two 20.50 and 22.50 m long road bridges used by cars and trucks in Bourg-lès-Valence (France) build in 2001 (Schmidt and Fehling, 2005). UHPC has also been subject of several research and development projects. Some topics covered in these projects include use of hybrid nano- and micro-scale reinforcement towards balanced improvement of the strength, toughness, impact and abrasion resistance, and durability characteristics of UHPC (Sbia et al., 2014b) (Sbia et al., 2014a) (Peyvandi et al., 2016), comparative evaluation of different discrete reinforcement systems in UHPC (Peyvandi et al., 2013), and assessment of the contributions of nanomaterials towards increasing the UHPC packing density (Sbia et al., 2015) and its bonding to steel reinforcement (Peyvandi et al., 2016).

The work reported herein focused on development of UHPC mix designs with a desired balance of packing density, water film thickness and paste film thickness for realizing high levels of compressive strength complemented with desired fresh mix workability. Packing density was raised through refinement of the gradation of all granular matter covering a broad length scale. The effects of water on packing density were accounted for, and viable ranges of water and excess paste film thicknesses for achieving desired fresh mix workability and effective binding of aggregates were identified. These criteria provided the basis for development of a systematic approach to UHPC mix design.

Packing density, water film thickness and paste film thickness

Given a unit volume filled with particles, packing density (or degree of packing) is defined as the volume of solids in a unit volume; it is equal to one minus the volume occupied by the voids. The packing density gives an indication of how efficiently particles fill a certain volume. If a high volume of aggregates is packed in a certain volume, the need for binder, which is usually expensive, to fill the voids and bind the particles will be decreased (Lange et al., 1997, Elrahman and Hillemeier, 2014, de Larrard and Sedran, 1994).

In the case of mono-sized spherical particles, packing density can reach 0.72 (Cumberland and Crawford, 1987). When particles are arranged in order, packing density tends to be higher for more spherical particles, and lower for more angular particles (Zou and Yu, 1996). When a proper amount of smaller particles is added to larger particles, the smaller particles would fill the voids between the larger particles and thus increase the packing density (Figure 1.1a). Excess amounts of smaller particles, on the other hand, would have a loosening effect on the packing of larger particles (Figure 1.1b). When the amount of smaller particles is not adequate, the larger particles would render a wall effect which undermine packing of the smaller particles (Figure 1.1c).

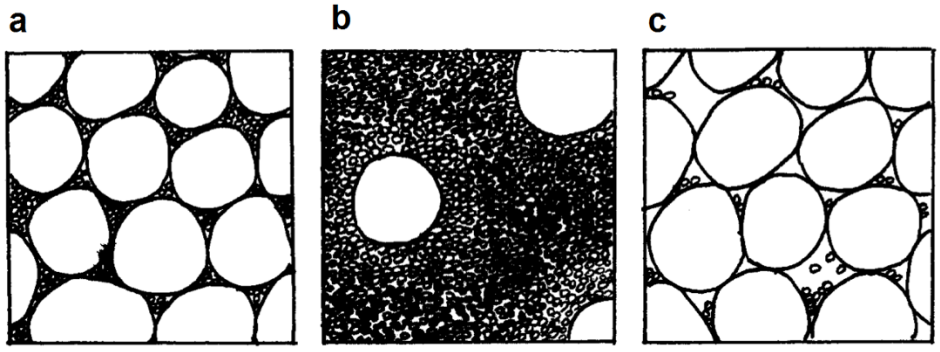

Figure 1.1. Filling effect (a), loosening effect (b), and wall effect (c) (Stovall et al., 1986)

Water plays a lubricating role in fresh concrete. For this purpose, all (cement and aggregate) particles in fresh mix should receive a continuous coating of water. The thickness of this water

film formed on particles is a key factor determining the fresh mix workability. In normal- and high-strength concrete materials, the available water fills the void space between particles, and also forms a continuous film on the particle surfaces (Figure 1.2). This is why the term 'excess water thickness' is used. In the case of ultra-high-performance concrete, the calculations conducted in this work indicate that the available water is not adequate to fill the voids between particles. Instead, all water seems to be adsorbed on the hydrophilic surfaces of particles, with the void spaces remaining empty. An optimum water film thickness should provide adequate workability without excessively separating the particles which would increase the porosity of the cementitious binder and thus lower its strength (Kwan and Fung, 2012, Kwan et al., 2010, Li and Kwan, 2011)

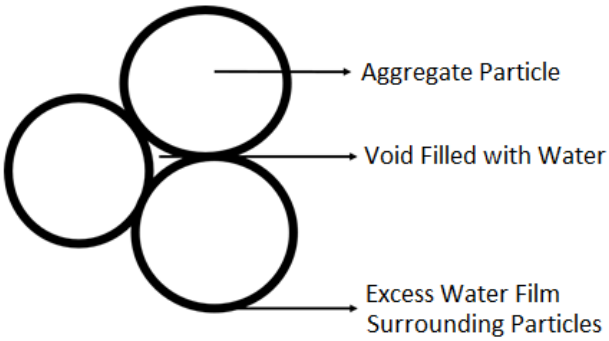

Figure 1.2. The excess water film thickness principle.

Given the brittle nature of the cementitious paste, it needs to fully coat the aggregates in order to render binding effects. For this purpose, paste should fill the void space between fine and coarse aggregates before it can effectively coat the aggregate particles. The excess paste theory views the thickness of the excess paste beyond that required for filling of voids between fine and coarse aggregates (Figure 1.3) as a parameter influencing the fresh mix and the hardened materials qualities. The cementitious paste in UHPC can reach higher strength levels than aggregates (Li and Kwan, 2013, Shen and Yu, 2011). This is not generally the case with normal- and high-strength concrete materials prepared with normal-weight aggregates. Therefore, new trends may emerge as

far as the relationship between the strength of UHPC and its excess paste film thickness is concerned.

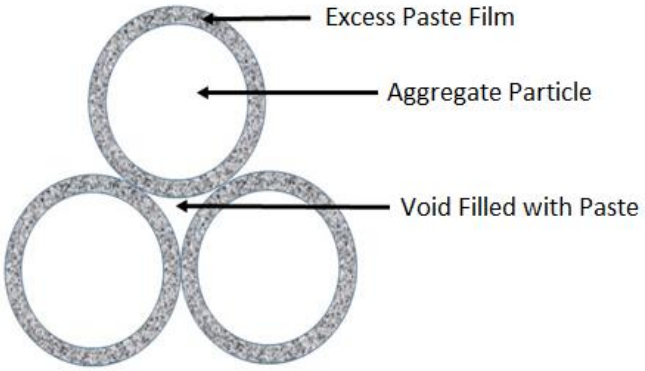

Figure 1.3. The excess paste film thickness principle.

The work reported herein derived viable ranges of fundamental mix parameters for ultra-high-performance concrete (UHPC). Achievement of these viable ranges can guide efforts to design UHPC mixtures with locally available materials.

Materials and Methods

Materials

Type I Portland Cement, undensified silica fume with ~ 200nm mean particle size, ~15m^2/g specific surface area and ≥105% 7-day pozzolanic activity index were used as raw materials. Slag, with specific gravity is in the range of 2.85 to 2.95 and bulk density varying from 1050 to 1375 kg/m^3, and limestone powder were the other raw materials used for preparation of ultra-high-performance concrete (UHPC) mixtures. Figure 1.4 presents the size distributions of all the powder materials (with micro- and nano-scale particle size) used in the project. Limestone with a maximum particle size of 12 mm was used as coarse aggregate. Two silica sands with different particle size were used as fine aggregates. Figure 1.5 presents the size distributions of the coarse and fine aggregates. A polycarboxylate-based superplasticizer (Chryso 150 supplied by Chryso)

and straight (brass-coated) steel fibers of 0.2 mm diameter and 12 mm length (supplied by Bekaert) were also used in UHPC mixtures.

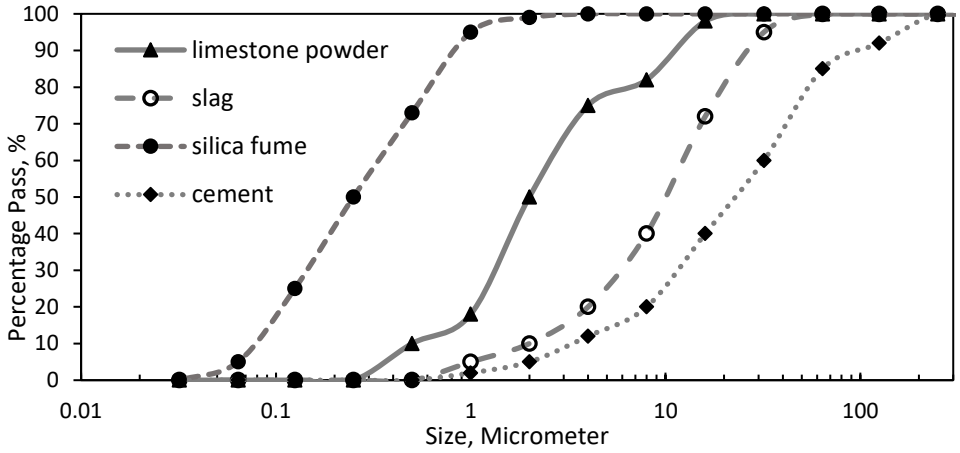

Figure 1.4. Particle size distributions of Type I Portland cement, limestone powder, slag and silica fume

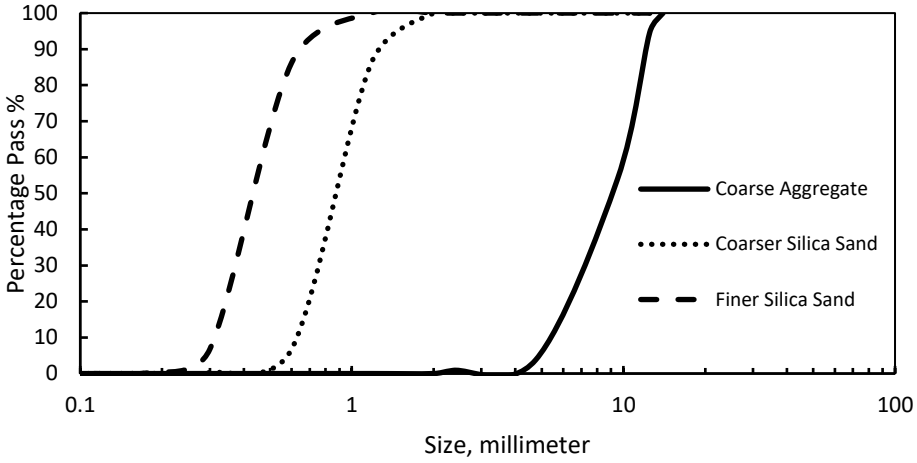

Figure 1.5. Particle size distributions of fine and coarse aggregates.

Mixing procedures

The ultra-high-performance concrete mixtures were prepared in the following steps:

1. Add all aggregates and powders to the mixer in the following sequence: coarse aggregate, fine aggregates, and powders (cement, silica fume, slag and limestone powder).
2. Dry-mix powders for two minutes.

3. Add water with half of the superplasticizer over two minutes, and mix for an additional half a minute.
4. Add the rest of the superplasticizer to the mix over one minute.
5. Continue mixing until a wet paste forms (usually 4 to 9 minutes)
6. Add the steel fibers to the mix.
7. Mix until a total mixing duration of 15 minutes is reached.

Calculations

Water film thickness

The conventional approach to water film thickness calculates the 'excess" water film thickness covering the surfaces of all granular matter, neglecting the amount of water required to fill the voids between the granules (Powers, 1969, Li and Kwan, 2013). For this purpose, the packing density of particles, Φ, needs to be calculated, based on which the void ratio between packed particles, μ, can be calculated as follows (Graybeal, 2011):

$$\mu = \frac{1-\Phi}{\Phi} \quad (1)$$

The excess water ratio(μ_w'), beyond that required to fill the void space, can thus be calculated as (Li and Kwan, 2013):

$$\mu_w' = \mu_w - \mu \quad (2)$$

μ_w is the total volume of water divided by the volume of all solid particles. The excess water film thickness, WFT, can then be calculated as WFT= μ_w'/As, where

$$As = \sum_{k=1}^{n} R_k . A_k \quad (3)$$

where, k refers to each of the n granular matter, R_k is the volumetric ratio of the k^{th} granular matter matter, and A_k is the specific surface area of the k^{th} granular matter.

While the above approach is valid for normal- and high-strength concrete, its application to ultra-high-performance concrete yields negative values of excess water film thickness. This indicates that, considering the very low water content of UHPC, the voids between granular matter cannot be filled with water. Given the energetic preference of water to adsorb onto hydrophobic surfaces, we assumed that water is present only as the film adsorbed on surfaces, and does not fill the voids. Hence, the water film thickness (WFT) can be calculated as follows for UHPC:

$$WFT=\mu_w/A_s \quad (4)$$

Paste film thickness

The paste film thickness is calculated as the thickness of the film formed on fine and coarse aggregates after the voids between aggregates are filled with the paste. For this purpose, considering the maximum wet packing density, $\Phi_{a,max}$, the minimum void ratio between aggregates to be filled with the paste is calculated as:

$$\mu_{min}=(1-\Phi_{a,max})/\Phi_{a,max} \quad (5)$$

The excess paste ratio μ_p' is then calculated as:

$$\mu_p' = \mu_p - \mu_{A\,min} \quad (6)$$

The excess paste film thickness can then be calculated as:

$$PFT = \mu_p' / A_A \quad (7)$$

Experimental optimization of mix proportions

A response surface design of experiments was developed for optimization of three primary mix proportioning parameters: (i) coarse aggregate-to-fine aggregate (weight) ratio; (ii) superplasticizer content; and (iii) steel fiber volume fraction. Viable ranges of these parameters were identified through a preliminary investigation. These ranges were 0.8-1.2 for coarse aggregate-to-fine aggregate ratio, 32 to 36 volume percent of total water for hydration for

superplasticizer content, and 1.5-2 vol.% for steel fibers. The response surface design of experiments for identifying the optimum combination of these variables is presented in Table 1.1 Besides these parameters, other aspects of the UHPC mix design were kept constant. The cementitious binder comprised Type I Portland cement: limestone powder: silica fume: slag at 48: 17: 24: 11 weight ratios. These cementitious materials were used at a constant dosage of 880 kg/m^3 in UHPC. The ratio of water to cementitious materials was also kept constant at 0.124.

Table 1.1. The response surface design of experiments for optimization of the UHPC mix proportions.

Mix No.	Coarse Aggregate, kg/m^3	Fine Aggregate, kg/m^3	Fiber, wt.% by all solids	SP, vol.% of Total Water for Hydration
1	1317.7	658.8	1.2	32
2	1317.7	658.8	1	34
3	1158.6	772.4	1	36
4	1158.6	772.4	0.8	32
5	1158.6	772.4	0.8	34
6	1158.6	772.4	0.8	36
7	1317.7	658.8	1	32
8	1158.6	772.4	1.2	34
9	1317.7	658.8	1.2	36
10	1317.7	658.8	0.8	32
11	1158.6	772.4	1.2	34
12	1158.6	772.4	0.8	36

Table 1.1 (cont'd)

13	1158.6	772.4	2	34
14	1158.6	772.4	2	34
15	1158.6	772.4	2	34

Experimental Results

Effect of the packing density on compressive strength

Figure 1.6 shows the relationship between compressive strength and packing density for ultra-high-performance concrete. The UHPC packing density is observed to range from 0.825 to 0.855. Within this range, compressive strength tends to increase with increasing packing density. This is the anticipated trend, noting that high superplasticizer contents are used in UHPC mixtures to achieve viable workability levels in spite of their low water contents.

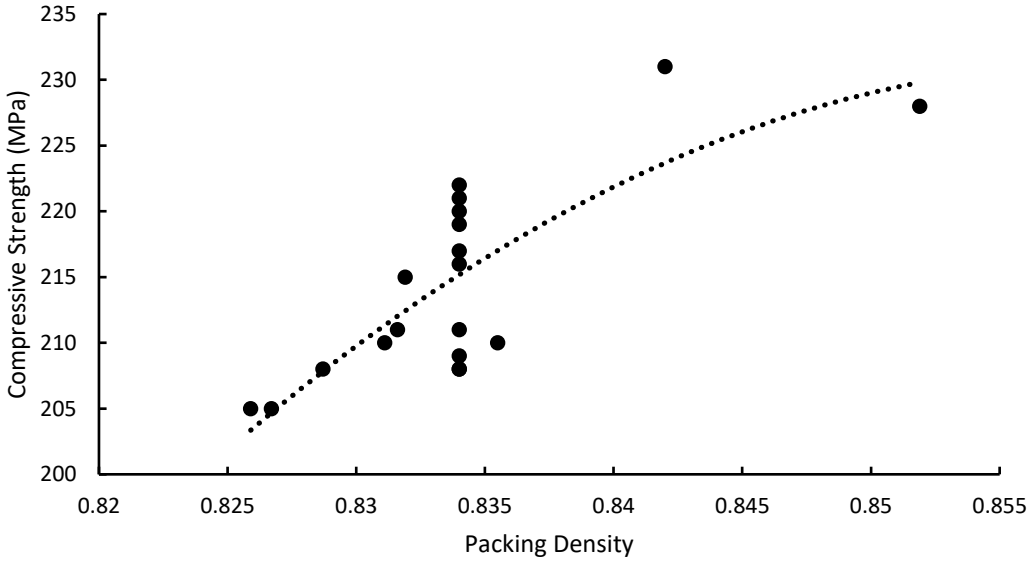

Figure 1.6. The relationship between compressive strength and packing density for UHPC.

Effect of the water film thickness on compressive strength

Figure 1.7 presents the relationship between the water film thickness and the compressive strength of the refined UHPC mix designs. The UHPC mixtures considered here have water film thicknesses ranging from 0.058 to 0.07 μm. Within this range, higher water film thicknesses yield lower values of compressive strength. It is worth mentioning that a minimum water film thickness would be required to lubricate the granular matter and produce a viable fresh mix workability. This minimum was probably exceeded in the UHPC mixtures considered here, which were designed to provide adequate workability. The calculated values of water film thickness for UHPC are lower than those reported for high-strength concrete. The use of relatively large superplasticizer dosages enabled lowering the UHPC water film thickness while still achieving adequate fresh mix workability.

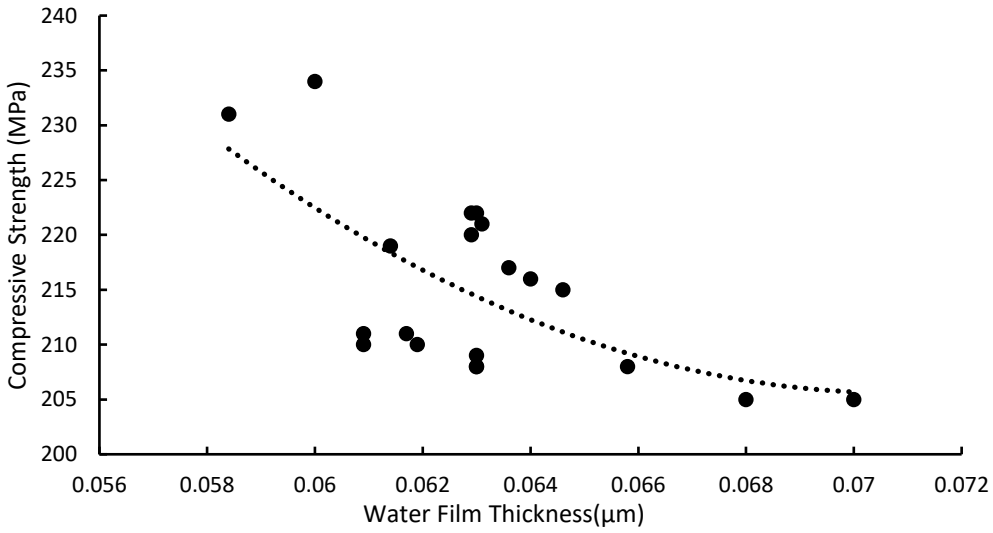

Figure 1.7. The relationship between water film thickness and compressive strength for UHPC.

Effect of the excess paste film thickness on compressive strength

Figure 1.8 shows the relationship between the UHPC compressive strength and the excess paste film thickness (on fine and coarse aggregates). The excess paste film thickness is observed to range from 220 to 280 μm for the UHPC mixtures considered here. The compressive strength of UHPC is observed to decrease with increasing excess paste film thickness. Similar to water film thickness, a minimum amount of excess paste film thickness would be required for achieving a viable level of fresh mix workability. This minimum was exceeded in the experimental work which sought to produce UHPC mixtures of adequate workability in fresh state.

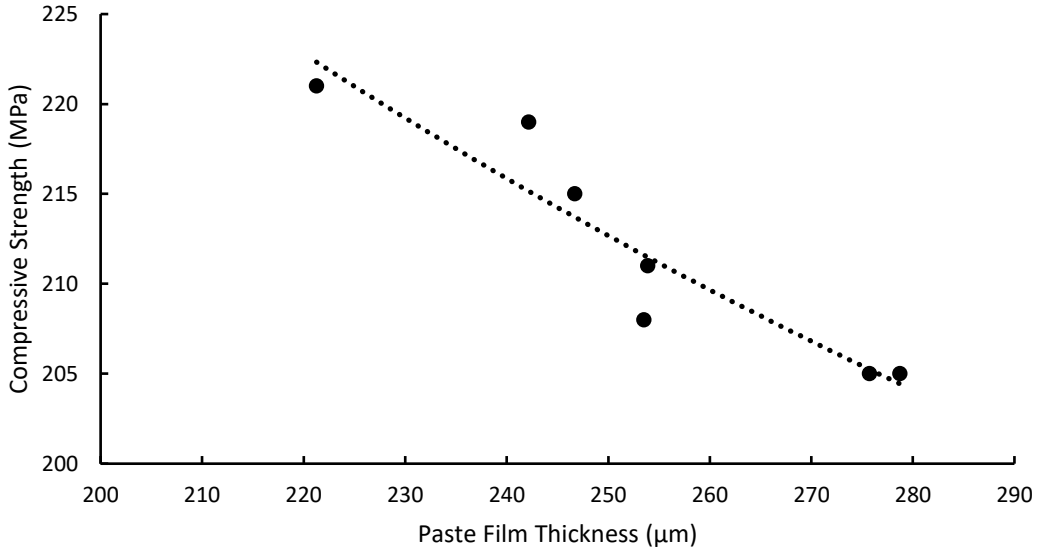

Figure 1.8. The relationship between the excess paste film thickness and the compressive strength of UHPC.

The response surfaces developed using the compressive strength and workability test data are presented in Figures 1.9 and 1.10, respectively. Response surface (Ridge) analysis of these test results yielded the following optimum levels (at 95% confidence) of the UHPC mix design variables:

Coarse to fine aggregate ratio: 1.20

Superplastizer dosage, vol. % 32.70

Fiber volume fraction, % 1.43

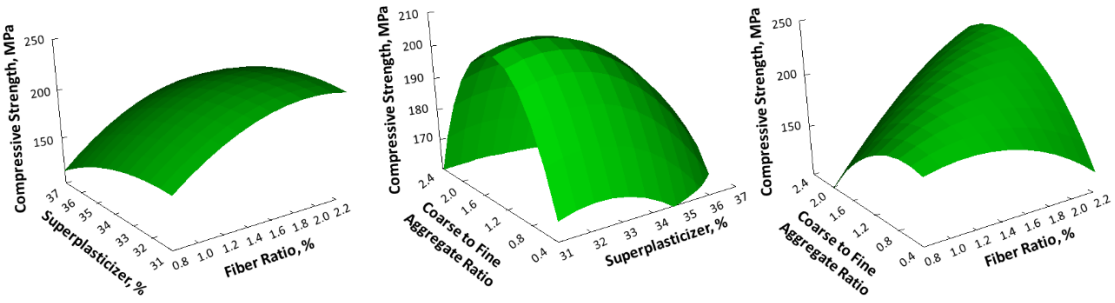

Figure 1.9. Response surfaces of the compressive strength test data generated in the optimization experimental program of the UHPC mix.

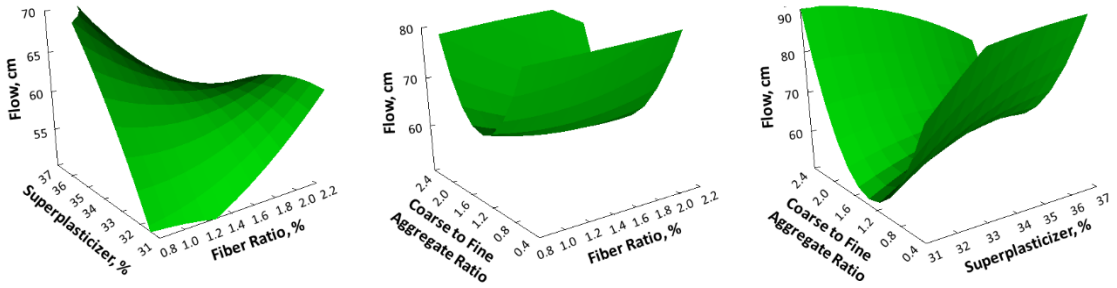

Figure 1.10. Response surfaces of the workability test data generated in the optimization experimental program of the UHPC mix.

The UHPC mix with the optimum mix design parameters identified above was prepared and subjected to steam curing procedures described earlier. Table 1.2 presents the calculated values of packing density, water film thickness (WFT), and excess paste film thickness (PFT) for the optimum mix; this table also presents the average values and ranges (for 8 tests) of flow and compressive strength. The average values of flow and compressive strength for the optimized mix were 68 cm and 223 MPa, respectively, which are within the ranges predicted by response surface. This finding point at the success of the optimization effort to identify a mix design that provides a desired balance of fresh mix workability and hardened concrete compressive strength. The

calculated values of packing density, water film thickness and excess paste film thickness for this optimized mix design are also within the viable ranges for ultra-high-performance concrete introduced earlier.

Table 1.2. The calculated values of packing density, water film thickness and excess paste film thickness, and the measured values of fresh mix flow and hardened concrete compressive strength for the optimized UHPC mix design.

Packing density	WFT, μm	PFT, μm	Fresh mix flow, cm	Compressive strength, MPa
0.843	0.053	219	68 ± 4	223 ± 8

Conclusions

A response surface design of experiments was developed for identifying the optimum values of coarse-to-fine aggregate weight ratio, superplasticizer content and steel fiber volume fraction in ultra-high-performance concrete. The material properties evaluated were the fresh mix flow and the hardened concrete compressive strength. For each UHPC mix design, the values of packing density, water film thickness and excess paste film thickness were also calculated. The following conclusions could be derived from test results for the ranges of variables considered in the experimental program

1. The UHPC packing density ranged from 0.825 to 0.855. Within this range, compressive strength increased with increasing packing density. This is the anticipated trend, noting that high superplasticizer contents are used in UHPC mixtures to achieve viable workability levels in spite of their low water contents.
2. The concept of excess water film thickness does not seem to apply to UHPC because the amount of water is not adequate to first fill the voids between granules before coating them. It is probable that all water assumes the energetically preferred form of adsorbed water.

Therefore, the commonly used excess water film thickness was replaced with water film thickness, assuming that all water was used to coat the granular matter. The UHPC mixtures considered in this investigation had water film thicknesses ranging from 0.058 to 0.07 μm. Within this range, higher water film thicknesses produced lower values of compressive strength. A minimum water film thickness would be required to lubricate the granular matter and produce a viable fresh mix workability. This minimum was probably exceeded in the UHPC mixtures considered here, which were designed to provide adequate workability. The calculated values of water film thickness for UHPC are lower than those reported for high-strength concrete. The use of relatively large superplasticizer dosages enabled lowering the UHPC water film thickness while still achieving adequate fresh mix workability. In order to achieve a desired balance of compressive strength and fresh mix workability, one can target water film thicknesses ranging from 0.-58 to 0.062 μm.

3. The excess paste film thickness ranged from 220 to 280 μm for the UHPC mixtures considered in this investigation. The compressive strength of UHPC decreased with increasing values of excess paste film thickness. Similar to water film thickness, a minimum amount of excess paste film thickness would be required for achieving a viable level of fresh mix workability. This minimum was exceeded in this experimental work which sought to produce UHPC mixtures of adequate workability in fresh state.
4. Response surface analysis of test results yielded optimum values of 1.5% for fiber volume fraction, 32-34% (by weight of water) superplasticizer content, and 1.2-1.4 coarse-to-fine-aggregate ratio. This optimum mix was prepared and tested; it yielded a desired balance of fresh mix flow and compressive strength (68 cm and 223 MPa, respectively). The calculated values of packing density, water film thickness and excess paste film thickness for this

optimum mix were 0.843, 0.053 μm and 219 μm, respectively, which occur within the viable ranges identified in the project. The measured values of flow and compressive strength were within the range anticipated through response surface analysis of the results of the optimization experimental program.

CHAPTER 2

Ultra-High-Performance Concrete: Fresh Mix Rheology and Fiber Dispersion Considerations

Abstract

Experimental investigations were conducted on the challenges that may be encountered in production of ultra-high-performance concrete (UHPC) using the commonly available rotary drum mixers. The rheological attributes of fresh UHPC mixtures were investigated, and a convenient set of tests were developed for field evaluation of the UHPC rheological attributes. These tests would allow for adjustment of the water content of the delivered UHPC to provide adequate workability characteristics, considering that the distinctly low water content of UHPC mixtures make them more prone to the adverse effects of the lack of control on the actual water content of concrete materials produced at industrial scale.

Introduction

Ultra-high-performance concrete (UHPC) is a relatively new class of advanced cementitious materials, with compressive and tensile strengths exceeding 150 MPa and 15 MPa, respectively (Aïtcin, 2011, Yu et al., 2015, Shi et al., 2015). UHPC mixtures are generally designed with relatively high dosages of silica fume, superplasticizer and steel fiber, relatively small concentrations of aggregates of small size, and Portland cement typically blended with fly ash or slag (Peyvandi et al., Van Der Putten et al., 2016). UHPC mixtures require extended mixing efforts to produce a homogenous and workable fresh mix; the sequence of addition of different mix ingredient could also influence the homogeneity of fresh mix. The high steel fiber content of UHPC can produce tendencies toward fiber balling, which tends to be more pronounced in large-scale production efforts. Figure 1 shows balls of steel fibers formed when UHPC is produced in a ready-

mixed concrete truck. There are also distinctions between the fresh mix rheology of UHPC versus normal-strength concrete that need to be considered in construction applications. UHPC incorporates high dosages of silica fume and superplasticizer, which could improportionally alter its (fresh mix) yield stress and viscosity(Šerelis et al., 2016, Van Der Putten et al., 2016). Relatively rapid loss of fresh mix workability is another consequence of the UHPC special mix design. This rapid loss of workability could be interpreted in field as rapid setting in spite of the fact that the high dosages of pozzolans and superplasticizer in UHPC mix designs lead to significant delay of set time(Yoo et al., 2016), which poses another challenge to construction practices which rely on timely setting of concrete to finish concrete surfaces(Sbia et al., 2017, Ghafari et al., 2015). Successful introduction of UHPC to mainstream construction applications would benefit from understanding and resolving the challenges associated with dispersion of fibers and the distinct features of its fresh mix rheology(Li et al., 2016, Wu et al., 2016).

Figure 2.1. Fiber balls produced in large-scale production of UHPC in a ready-mixed concrete truck.

Figure 2.2 shows a core taken from a large UHPC placement where mixing was accomplished in a ready-mixed concrete truck. Formation of fiber balls is apparent in this figure.

Fiber balling is a challenge in scale-up of UHPC production using conventional concrete mixing practices. The selection of fiber type and volume fractions should be made to balance desired engineering properties of UHPC against the potential for fiber balling in large-scale production of UHPC. The work reported herein focused on selection of steel fiber types which reduce the tendency towards balling and also provide desirably high values of compressive strength. It is worth mentioning that, unlike normal- and high-strength concrete, reinforcement with properly selected discrete fibers can produce a significant rise in compressive strength (Scott et al., 2015).

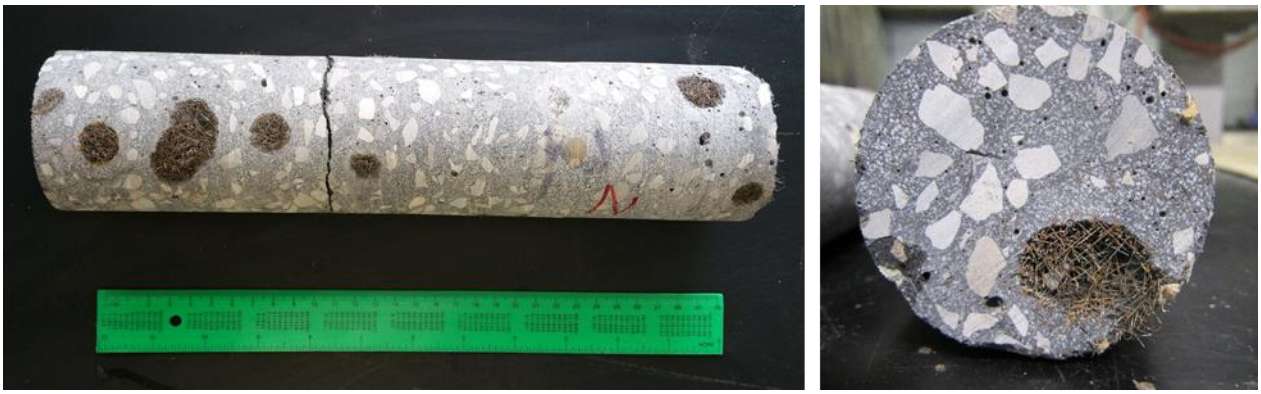

Figure 2.2. Pictures of a UHPC core and its cross-sections taken from a large UHPC placement where mixing was performed in a ready-mixed concrete truck.

UHPC mixtures incorporate high dosages of superplasticizer for lowering their water/cementitioius ratio while retaining desired fresh mix workability (Zhang et al., 2016, Li et al., 2016).

Given the low water content of UHPC mixtures, the uncertainties with water content in industrial-scale production caused by, say, variabilities in the aggregate moisture content, could have more pronounced effects on the fresh mix rheology of UHPC when compared with normal-strength concrete. This would require thorough assessment of the UHPC fresh mix rheology in field conditions (Choi et al., 2016). The rheometers which can make such thorough measurements,

however, do not suit filed applications (Choi et al., 2013a, Choi et al., 2013b). UHPC mixtures also exhibit relatively high levels of surface adhesion which could, through interactions with formwork and reinforcing steel, challenge their field placement and consolidation (Lowke, 2009). There is thus a need for assessment of the surface adhesion attributes of UHPC in field.

The work reported herein focused on addressing the UHPC fresh mix qualities which challenge its transition to mainstream construction practices. Methods were devised for resolving the fiber balling problems, and test procedures suiting field applications were developed for thorough assessment of the fresh mix rheology and surface adhesion characteristics.

Materials

The granular raw materials used in the UHPC mix design considered in this investigation can be divided into two categories: (1) cementitious materials and fine filler (limestone powder); and (2) aggregates. The cementitious materials and the fine filler considered in this investigation were: (i) Type I Portland cement; (ii) undensified silica fume with ~200 nm mean particle size, ~15 m^2/g specific area and >105% 7-day pozzolanic activity index; (iii) ground granulated blast furnace slag with specific gravity of 2.9 and bulk density of 1,200 kg/m^3, ground to less than 45 micrometer particle size; and (iv) limestone powder with 2 micrometer mean particle size. The particle size distributions of cementitious materials and limestone powder are presented in Figure 3. The aggregates used in UHPC mixtures included (see Table 1 for size distributions): (i) limestone coarse aggregate with 12 mm maximum size; (ii) coarse silica sand with mean particle size of 0.8 mm and specific gravity of 2.67; and (iii) fine silica sand with mean particle size of 0.4 mm and specific gravity of 2.65. A polycarboxylate-based superplasticizer (Chryso 150 supplied by Chryso, with 1.06 specific gravity and 30% solid content) was used in UHPC mixtures. The steel fibers used in UHPC mixtures are introduced in Table 2.2; those with 0.2mm diameter were brass-coated.

These broad varieties of fibers were considered because the effect of fiber selection and blending on fiber balling was found to be significant.

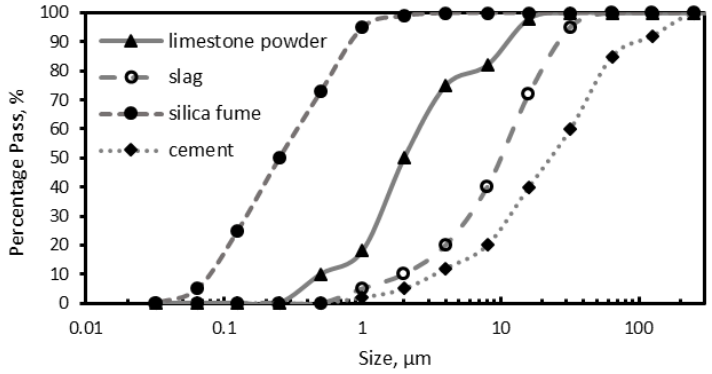

Figure 2.3. Particle size distributions of cementitious materials and limestone powder.

Table 2.1. Particle size distributions of aggregates.

Sieve Size, mm	Percentage Pass, %		
	Coarse Aggregate	Coarser Sand	Finer Sand
0.15	0	0	0.05
0.18	0	0.1	0.3
0.30	0	0.3	6.8
0.60	0	6.7	86
1.18	0	86	100
2.00	0	100	100
2.360	0.9	100	100
4.750	3.8	100	100
9.500	54	100	100

Table 2.1 (cont'd)

12.500	95	100	100

Table 2.2. The fiber types used in UHPC mixtures.

Name	Diameter, mm	Length, mm	Supplier
Small steel fiber	0.2	13	Bekeart
Medium steel fiber	0.2	30	Bekeart
Glued fiber	0.55	30	Bekeart
Hooked fiber	1	60	Bekeart
Glass fiber	0.1	19	Buddy Rhodes
Carbon Fiber	1	15	Zoltek

The UHPC mix design considered in this investigation is presented in Table 3 together with the mix design of a normal-strength concrete used in the project for comparison purposes. A Portland cement paste with water/cement ratio of 0.40 was also used as control in viscosity tests, with similar tests performed on the paste content of UHPC.

Table 2.3. UHPC and normal-strength concrete mix designs.

Material	Quantity, kg/m^3	
	UHPC	Normal Strength Concrete
Coarse aggregate	612	1080
Coarser silica sand	500	960

Table 2.3 (cont'd)

Finer silica sand	500	-
Cement	604	360
Silica fume	268	-
Slag powder	120	-
Limestone powder	216	-
Water	144	198
Superplasticizer	57.6	-
Steel fiber	148	-

Methods

Ultra-high-performance concrete mixtures were prepared in the following steps using a rotary drum mixer of 0.035 m^3 capacity (Figure 2.3):

1. Add all aggregates and powders to the mixer in the following sequence: coarse aggregate, fine aggregates, and powders (cement, silica fume, slag and limestone powder).
2. Dry-mix for two minutes.
3. Add water with half of the superplasticizer over two minutes, and mix for an additional half a minute.
4. Add the rest of the superplasticizer to the mix over one minute.
5. Continue mixing until a wet paste forms (usually 4 to 9 minutes).
6. Add the steel fibers to the mix.
7. Mix until a total mixing duration of 15 minutes is reached.

Fiber ball formation typically occurs after the addition of fibers (Step 6) when fiber fibers of 0.2mm diameter and 13-15mm length are used. The approach evaluated in this project for resolving the fiber balling problem involved use of different types (including blends) and volume fractions of steel fibers. The focus was on resolving the fiber balling problem without compromising the compressive strength of UHPC.

Figure 2.4. The laboratory-scale rotary drum mixer used in this investigation.

Three aspects of the fresh UHPC mix behavior need to be evaluated: yield stress, viscosity and surface adhesion. The test procedures devised for measurement of these properties are shown in Figure 2.5. All these tests use rectangular Ti-Al alloy steel plates of No. 6 surface roughness (ASTM A480). The plate used in surface adhesion test (Figure 2.5a) had planar dimensions of 9cmx11cm and a thickness of 0.2 cm. The plates used in push-in (Figure 2.5b) and pull-out (Figure 5c) tests were similar, with 10cmx15cm planar dimensions and thickness of 0.2 cm. The locations of holes used for handling the plates in surface adhesion and push-in/pull-out tests are shown in Figure 2.6. The surface adhesion test (Figure 2.5a), inspired by a research reported in the literature (Adhikari et al., 2001), involves pushing the plate onto the fresh concrete surface until a full contact (including at all four corners) is established between the plate and the concrete surface. The plate is then moved away from the concrete surface at a speed of 1 cm per second. The maximum force required for separation of the plate from the surface is recorded as an indication of the surface adhesion qualities of the fresh concrete mix. Figure 2.7 shows the separation mechanism of the

plate from the mass of fresh concrete in the surface adhesion test. The force required to separate two objects that are not permanently bound together is a measure of tack. Tackiness is often addressed to character the surface adhesion of sticky material. Pull resistance between two surfaces and stated that cohesion, surface tension and viscosity all contribute to the tack. A material is sticky when the energy required to break its bond with a surface is as large as the interfacial energy that comes from the dissipation during the separation process, which in turn causes deformation and friction in the contact film.

In the push-in test (Figure 2.5b), which provides an indication of the fresh mix viscosity (Draijer, 2007), the plate is pushed vertically into concrete at a speed of 1 cm per second, and the maximum force required for pushing the plate into concrete until the hole shown in Figure 2.6b) reaches the concrete surface is recorded. The resistance to push-in action is provided by the glazing of aggregates against the plate and also the flow. The concrete with good consistency has a low viscosity, this is a viscosity which is close to the viscosity of water, when there will be high amount of coarse aggregate the aggregate can glaze the plate wall if the consistency is too low; when there will be too many fines present the flow friction will be high as well. A higher pressure is needed to push the concrete through the pipes which will increase the risk for bleeding or segregation.

In the pull-out tests (Figure 2.5c), which provides an indication of the fresh mix yield stress (Zhang et al., 2010), noting that the presence of high percentage of fine particles in UHPC provides for a non-Newtonian behavior of its fresh mix. The shear stress at which the material starts flowing is called yield stress(Zhu and De Kee, 2006, Zhu et al., 2001). After waiting for 5 seconds, the plate is pulled out of the fresh concrete at a speed of 1 cm per second, and the maximum force required for complete removal of the plate from concrete is recorded. The device submerged into a test material, which indicated UHPC in this paper; the plate is slowly pulled out of the suspension

while measuring the required load, which comes from the resistance of the material to this motion. To obtain the true yield stress, the shearing action should be within the material and not between the material and an object, such as a plate. Therefore, ideally, a virtual plane of material should be moved inside the suspension and the material-material shearing stresses measured. This option, however, is not available in a simple test for field applications. The yield stress obtained in this pull-out test was always larger than the surface adhesion force obtained via the test procedure shown in Figure 2.5a.

(a)Surface Adhesion Test (b) Push-In Test (c) Pull-Out Test

Figure 2.5. The three tests devised for thorough measurement of the fresh UHPC mix properties.

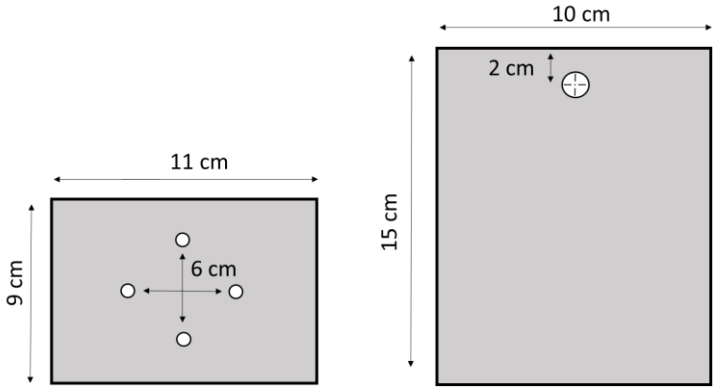

Figure 2.6. Locations of the holes used for handling of the plates in surface adhesion (left) and push-in/pull-out (right) tests.

In order to measure the rheological features of fresh UHPC pastes (and also those of the control Type I Portland cement paste), a digital rheometer (DV-III ULTRA) with stress control and data

acquisition capabilities was used (Figure 2.7a). This apparatus measures the shear yield stress and plastic viscosity of fresh concrete mixtures. The fresh mix was placed in a sample holder comprising an external sleeve and an internal rotator (spindle). The dimensions of the internal rotator and the external sleeve can be selected based on the rheological properties of the fresh mix. The container used in this investigation had 600 ml capacity with a working volume of 500 ml; ae standard Lv5 spindle (Figure 2.7b) was selected for use in this investigation after preliminary trials. A stress controller is used in this test to control the torque of the internal rotator (spindle). If the relationship between torque and rotational speed is linear, then the linearity coefficients are proportional to the Bingham constants of the fluid.

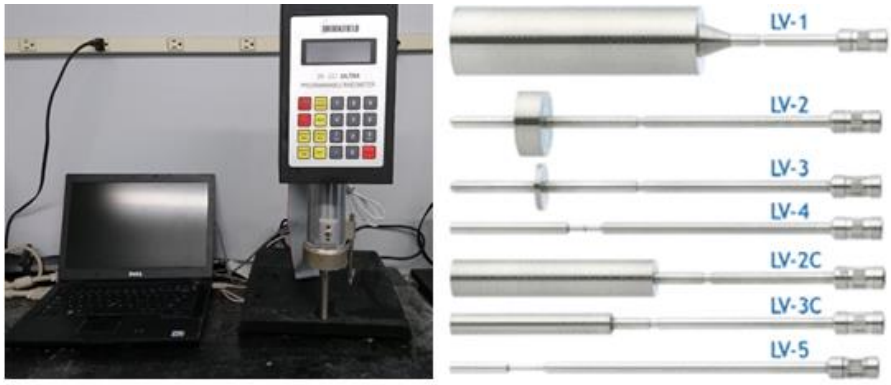

Figure 2.7. The rheometer and the spindles (LV-5 was selected after preliminary trials) used in this investigation.

The fresh mix flow test was also measured per ASTM C1611 Besides the tests performed on fresh concrete mixtures, 50 mm cube specimens of UHPC were also cast into moles and consolidated via external vibration. The specimens were demolded after 24 hours of storage in sealed condition, and were subjected to steam curing at 90^{o}C for 48 hours. The cured specimens were then stored at

50% relative humidity and room temperature, and subjected to compression tests per ASTM C39 at 7 days of age.

Results and Discussion

Balling of Steel Fibers

Figure 2.8 shows the steel fiber balls formed during mixing of the base UHPC mix design of Table 3 prepared with brass-coated steel fibers of 0.2 mm diameter and 13 mm length in a laboratory-scale rotary drum mixer. The fiber balls comprised steel fibers, cementitious materials, minor quantities of fiber aggregates with hardly any coarse aggregates, steel fiber balls were formed and each was separated and with force resistance. This fiber balls were combined with fiber, cementitious materials and little coarse aggregate. The resulting UHPC balls, excluding the fiber balls, provided 7-day compressive strength of 224 ± 4MPa (based on tests on four cube specimens).

Figure 2.8. The steel fiber balls formed in drum mixer.

The high specific surface area of glass fibers raised the water requirement of the mix by 20%. In spite of this rise in water content, still had a dry consistency (dynamic flow of 12cm), and exhibited a tendency towards formation of pellets comprising largely of the cementitious paste (Figure 2.10). The resultant concrete produced a relatively low compressive strength of 122 ± 6 MPa.

Figure 2.9. The cementitious paste pellets formed in drum mixer for the UHPC mix with glass fiber reinforcement.

The extra water required to produce a flow of 14cm was 10% of the original water content. The compressive strength achieved with carbon fibers was still low at 138.5± 5MPa.

Figure 2.10. The cementitious paste pellets formed in drum mixer for the UHPC mix with carbon fiber reinforcement.

The use of glued steel fibers resolved the problem with fiber balling; (Figure 2.11) however, about 45% of fibers remained glued together and did not separate. Furthermore, the dissolution of the water-soluble glue in UHPC produced a viscous fresh mix with compromised workability. This can be attributed to the high dissolved concentration of the glue in the mixing water, considering that UHPC mixtures have distinctly low water contents. The compressive strength achieved with glued steel fibers was relatively low at 133.56 ± 5 MPa.

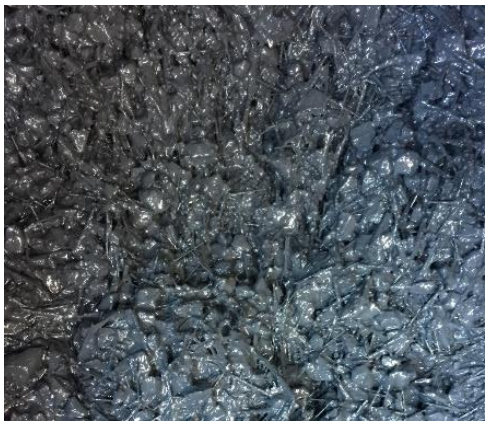

Figure 2.11. The fresh UHPC mix prepared with glued steel fibers.

When half of the steel fibers with 0.2 mm diameter and 13 mm length were replaced with hooked fibers of 1 mm diameter and 60 mm length, the problems with formation of steel fiber balls and cementitious paste pellets were resolved. The fresh mix also provided a desired flow of 16cm The compressive strength provided by the mix was 176± 4 MPa that is reasonably high (qualifying the material as UHPC) but steel lower than that achieved with only small steel fibers used in the mix (after removal of the fiber balls).

Figure 2.12. The fresh UHPC mix appearance in drum mixer when 50% of fine steel fibers are replaced with coarse (hooked) steel fibers.

Replacement of 50% of fine (0.2 mm diameter by 13 mm length) steel fibers with steel fibers of medium size (0.2 mm diameter by 30 mm length) also was effective in resolving the fiber ballig problem while providing a desired fresh mix workability represented by a flow of 18cm cm (that

is better than that achieved with 100% finer fibers) and a desirably high compressive strength of 198.5± 3 MPa. These are the best balance of fresh mix and hardened material qualities produced in this work, suggesting that a combination of fine and medium steel fibers and equal weights offers a viable solution to the fiber balling problem (without producing a tendency towards compromised fresh mix workability and formation of cementitious paste pellets).

Figure 2.13. The fresh UHPC mix appearance in drum mixer when 50% of fine steel fibers are replaced with medium-sized steel fibers.

An attempt was made to reduce the replacement level of fiber fibers with medium fibers in order to raise the UHPC compressive strength. A fiber blend comprising 75% fine and 25% medium fibers also did not exhibit any visual indications of fiber ball formation after 20 minutes of mixing (Figure 2.14). There were a minor tendency towards fiber balling after 15 minutes of mixing, which was resolved with 5 more minutes of mixing. The fresh mix flow was calculated at 17 cm, and the resulting compressive strength was 210 ± 3 MPa. While this blend of steel fibers seems to be preferred, one should be concerned about the scale-up effects from a laboratory-scale to an industrial-scale drum mixer. Our field experience points at an increase tendency towards fiber balling in a ready-mixed concrete mixer when compared with a laboratory-scale drum mixer.

Figure 2.14. The fresh UHPC mix appearance in drum mixer when 25% of fine steel fibers are replaced with medium-sized steel fibers.

Fresh Mix Rheology

Figure 2.15 shows the variation of viscosity with shear rate for the UHPC and Portland Cement pastes. Viscosity of the UHPC paste is observed to be much higher than that of the Portland cement paste especially in the lower rage of shear rate. For both pastes, viscosity decreases with increasing shear rate. The shear stress-shear rate relationships shown in Figure 2.16 indicate that shear stress increases with shear rate at a significantly higher rate for UHPC than for normal Portland cement paste. The resultant values of viscosity and yield stress are presented in Table 4 for the UHPC paste and the normal Portland cement paste. The yield strength of the UHPC and normal Portland cement paste are observed to be comparable; the viscosity of the UHPC paste, on the other hand.

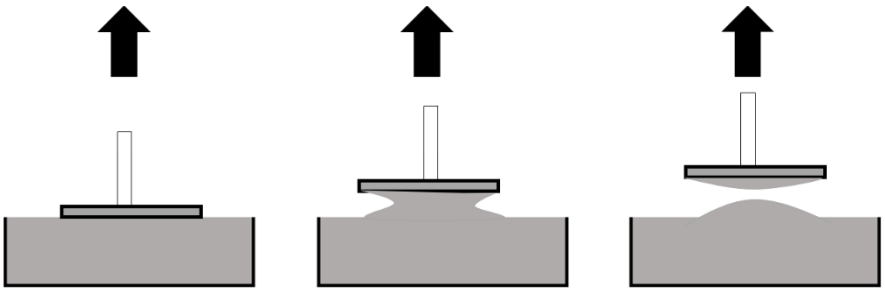

Figure 2.15. Separation mechanism of the plate from the mass of fresh concrete in the surface adhesion test

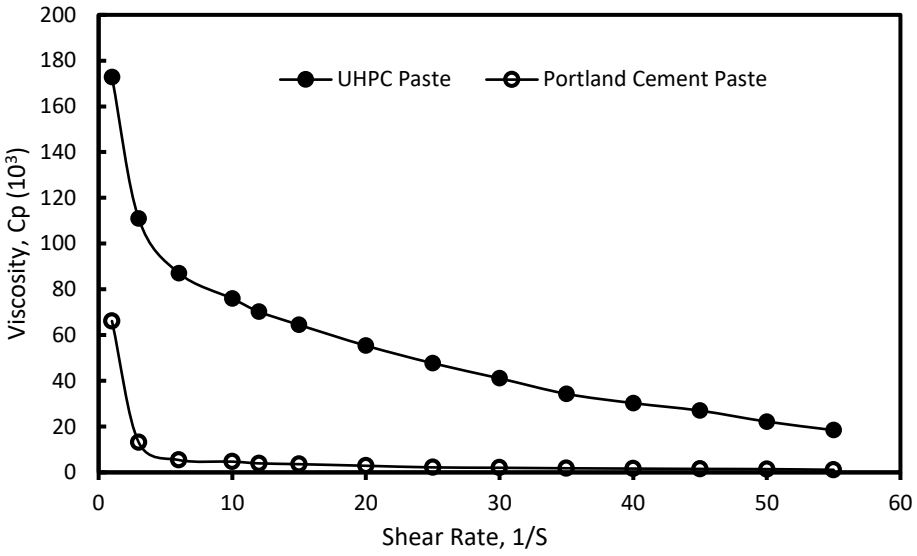

Figure 2.16. The viscosity-shear rate relationships for the UHPC and normal cement pastes.

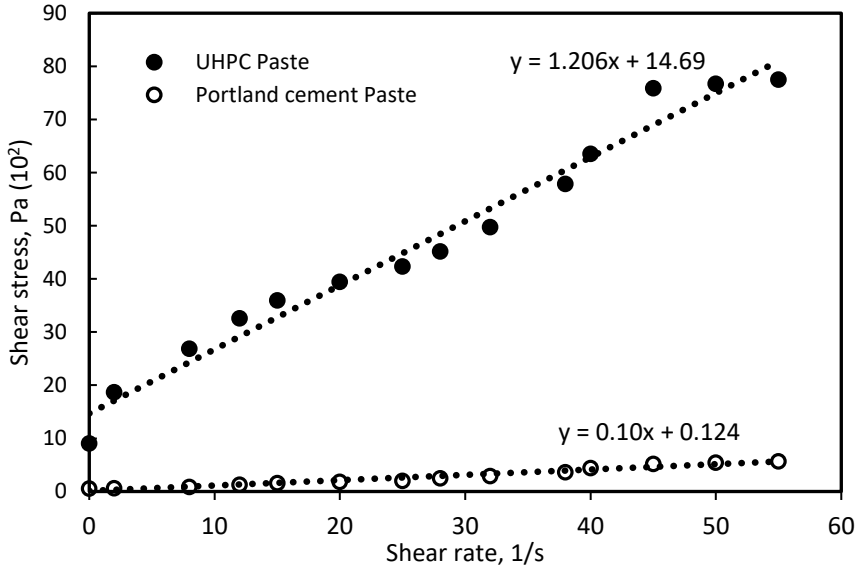

Figure 2.17. The shear stress-shear rate relationships for the UHPC and normal cement pastes.

Table 2.4. Measured values of viscosity and yield stress for the UHPC paste and the normal cement paste.

	Portland cement paste	UHPC paste
Viscosity, Pa	12.40	1469

The simple surface adhesion, pull-out and push-in tests were used to investigate the effects of water content on the UHPC rheology. The surface adhesion force seems to peak at an intermediate value of water content (Figure 2.18), while the pull-out force (correlating with yield strength) and the push-in force exhibit, as shown in Figures 2.19 and 2.20, respectively, general trends towards lower values with increasing water content). There are variabilities in these trends (especially in push-in tests) that point at the need for establishing the variances of test results and specifying a minimum number of replicated tests to be performed on the fresh mix.

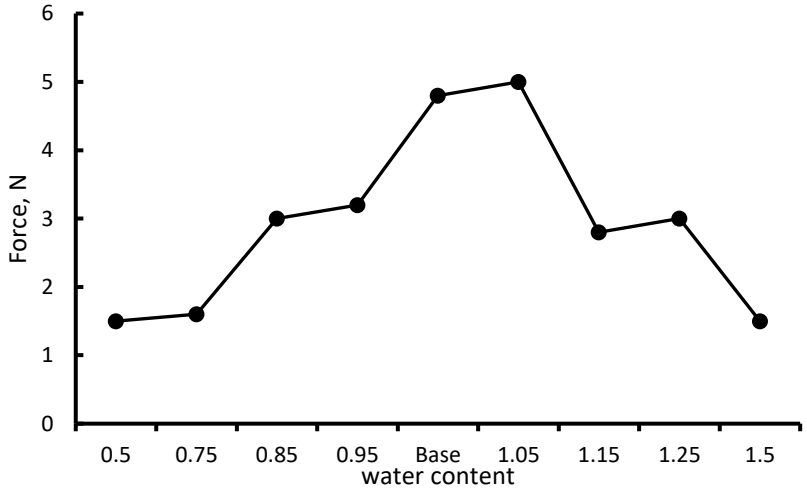

Figure 2.18. Effect of the UHPC water content of the surface adhesion force.

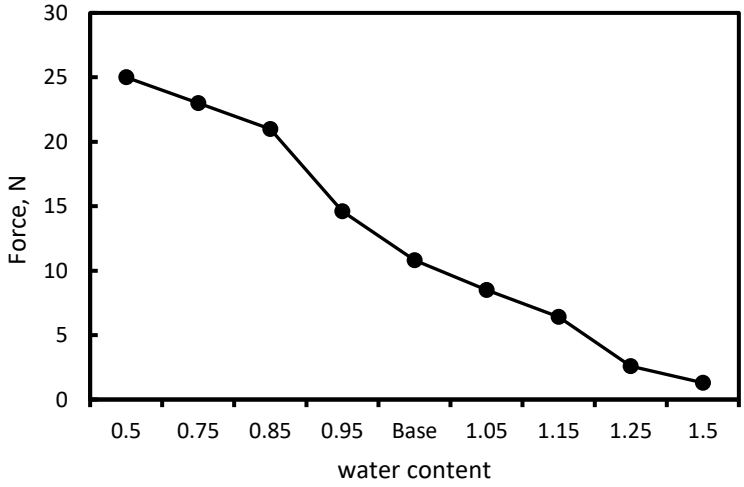

Figure 2.19. Effect of the UHPC water content on the pull-our force.

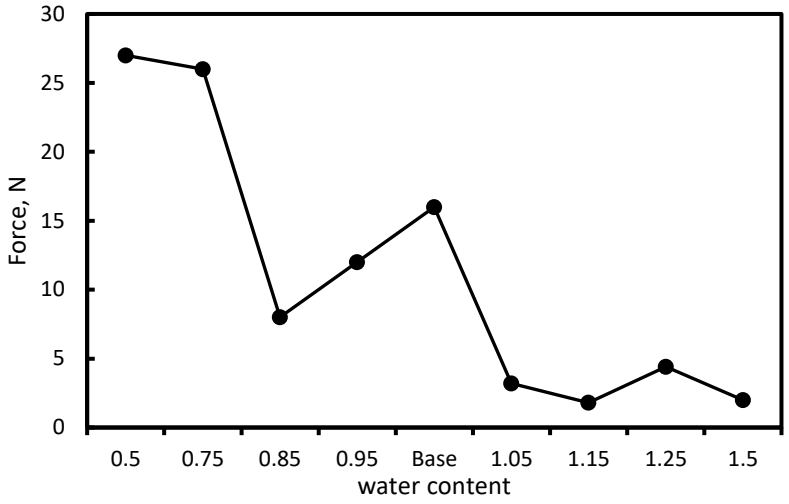

Figure 2.20. Effect of the UHPC water content on the push-in force.

Images captured from the top surfaces of UHPC mixtures with different water contents indicate that excessively high water contents (20% less than that in the base UHPC mix) lead to settlement of coarse aggregates (Figure 2.21a) while excessively low water contents (20% less than that in the based UHPC mix) challenge uniform dispersion of the coarse aggregates (Figure 2.21b). While the base UHPC mix produced a compressive strength of 224 MPa. Increasing and decreasing the water content by 20% (Figures 2.21a and 2.21b, respectively) lowered the compressive strength to 182 MPa and 208 MPa, respectively.

(a) Excess water (b) Base mix (c) Insufficient water

Figure 2.21. Surface appearances of UHPC mixtures with different water contents.

Conclusion

1. Relatively high steel fiber contents are commonly used in ultra-high-performance concrete (UHPC) mixtures in order to enhance their ductility and strength. Specialized mixing procedures are employed to ensure the homogeneity of UHPC mixtures and ensure thorough dispersion of steel fibers. Production of UHPC in commonly used drum mixers, however, produces tendencies towards fiber balling. These tendencies tend to be more pronounced in industrial-scale production of UHPC (e.g., in ready-mixed concrete trucks). Investigations were conducted in order to resolve the fiber balling problem encountered in production of UHPC using drum mixers. The options considered included the use of glass and carbon fibers in lieu of steel fibers, and blending of steel fibers of different size. Glass and carbon fibers raised the water content (for achieving adequate fresh mix workability) and lowered the compressive strength of UHPC. Blending of fine and coarse steel fibers (in lieu of the fine fibers commonly used in UHPC) was effective in resolving the fiber balling problem. This investigation was conducted using a laboratory-scale drum mixer. The blends of fine and coarse fibers considered in this investigation produced compressive strengths that were only slightly below those obtained with fine fibers, but mitigated the fiber balling problem.
2. Investigations into the rheological attributes of the UHPC paste versus a normal Portland cement paste indicated that the yield strength of UHPC paste is comparable to that of that normal Portland cement paste; its viscosity, however, is two orders of magnitude greater than that of the Portland cement paste. Fresh mix workability tests (e.g., slump) that reflect primarily the yield strength of fresh concrete mixtures could thus produce misleading results in application to UHPC. A set of convenient tests were developed for field

assessment of the fresh mix rheology of UHPC. These tests quantify three aspects of the fresh UHPC performance that relate to its viscosity, yield strength and surface adhesion capacity. Correlations were drawn between the water content of UHPC and the results of these three tests. These correlations would allow for adjustment of the water content of the delivered UHPC prior to pouring. The tests are rapid, and are designed for field application. They would allow for resolving the uncertainties with water content of UHPC mixtures that are produced using industrial-scale concrete batching and production facilities.

CHAPTER 3

Improvement of the Surface Quality and Aesthetic of Ultra-High-Performance Concrete

Abstract

The low moisture content of ultra-high-performance concrete (UHPC) combined with its minimal bleeding lead to quick drying of its exposed surfaces via moisture evaporation and self-desiccation. The result is formation of a rough texture and cracks on the exposed surfaces of UHPC within hours after its placement and finishing. This phenomenon is occasionally referred to as 'elephant skin' formation. Alternative strategies were devised and experimentally evaluated for control of elephant skin formation. These strategies emphasized reduction of moisture loss from the surface, enhancement of dimensional stability, and increase of plastic shrinkage crack resistance. The potential for elephant skin formation was assessed through monitoring of the surface penetration resistance, temperature, crack area and aesthetics under exposure to air flow and radiation. The results indicated the measures which effectively reduce moisture loss from the surface are most effective in controlling elephant skin formation on the exposed surfaces of ultra-high-performance concrete.

Introduction

Ultra-high-performance concrete (UHPC), which compressive strengths exceeding 250 MPa,(Shi et al., 2015) (Richard and Cheyrezy, 1995, Russell and Graybeal, 2013, Schmidt et al., 2004, Richard, 1996)are produced with high contents of cementitious materials, low ratios of water to cementitious materials (0.15 to 0.20), and aggregates of relatively small particle size(Richard and Cheyrezy, 1995); they exhibit higher rates of shrinkage (Holt, 2005). The low moisture content of UHPC combined with its high barrier qualities lead to quick drying of its surfaces due to moisture loss to evaporation and self-desiccation (Bentur et al., 2001), combined with minimal bleeding of

UHPC. The result is a surface of rough texture which can exhibit microcracking (Uno, 1998). Figure 3.1a shows an example UHPC surface upon finishing. The appearance of the same surface after 24 hours is shown in Figure 3.1b where a rough surface texture with some cracking is noted. This surface texture is occasionally referred to as elephant skin.

Figure 3.1. Development of a rough UHPC texture with some cracking 24 hours after placement.

Formation of ‘elephant skin’ is not pronounced on the surface of small laboratory specimens, although it can be detected on the surfaces of medium-scale slabs prepared in laboratory. As field applications of UHPC increase, however, this tendency towards elephant skin formation cannot be neglected. Different strategies were devised for preventing elephant skin formation on UHPC surfaces.(Shi et al., 2015, Soroushian et al., 1993, Yang et al., 2005, Acker and Behloul, 2004) These strategies emphasized reduction of moisture loss from surface,(Graybeal, 2006, Goldman and Bentur, 1994) enhancement of the surface ductility, shrinkage control(Banthia and Gupta, 2006, Soroushian and Ravanbakhsh, 1998, Cohen et al., 1990), and introduction of discrete reinforcement systems(Altoubat and Lange, 2001). While elephant skin formation on UHPC surfaces is highly pronounced and can occur in different climatic conditions, it may be compared with plastic shrinkage cracking (Holt, 2005)of normal concrete which is occasionally observed in

climatic conditions which promote rapid surface drying (e.g., windy and dry conditions) (Torrenti et al., 1999, Ravina and Shalon, 1968, Wang et al., 2001).

Research and Significance

Ultra-high-performance concrete (UHPC) offers significant advantages in terms of mechanical performance, durability, sustainability, structural efficiency and life-cycle economy. Field applications of UHPC, however, encounter problems associated with the formation of exposed surfaces of rough texture and reduced quality. The work reported herein focuses on the resolution of the surface problems of UHPC. This would enable effective use of the advantages offered by UHPC in construction of infrastructure systems.

Materials and methods

A host of materials and methods were employed to resolve the UHPC surface problems. The materials and methods employed in this work are presented below under two categories: (i) base uhpc materials and methods; and (ii) materials and methods employed for resolving the UHPC surface issues.

Base UHPC Materials and Methods

The cementitious and fine filler materials used for production of UHPC included: (i) Type I Portland Cement; (ii) undensified silica fume with ~200nm mean particle size, ~15m^2/g specific area, ≥105% 7-day pozzolanic activity index; (iii) ground granulated blast furnace slag with specific gravity of 2.9 and bulk density of 1,200 kg/m^3, ground to less than 45 micrometer particle. The aggregates used in UHPC mixtures included (see Figure 3.3 for particle size distributions): (i) limestone coarse aggregate with 12 mm maximum size; (ii) coarse silica sand fine aggregate with specific gravity of 2.65; and (iii) fine silica sand fine aggregate with specific gravity of 2.65. A

polycarboxylate-based superplasticizer (Chryso 150 supplied by Chryso, with 1.06 specific gravity and 1.8% solid content) and steel fibers of 0.2mm diameter and 15mm length with brass coating (supplied by Bekaert) were also used in UHPC mixtures. The base UHPC mix design considered in this investigation is presented in Table 3.1.

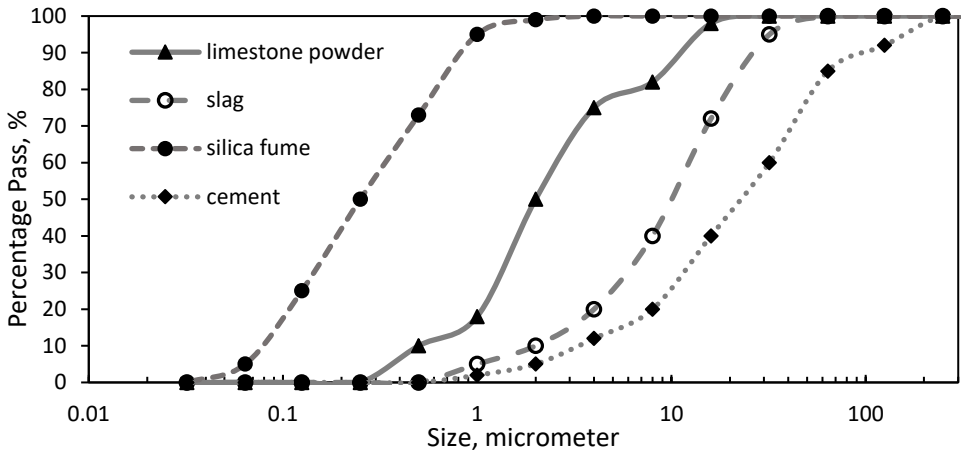

Figure 3.2. Particle size distributions of the cementitious materials and limestone powder.

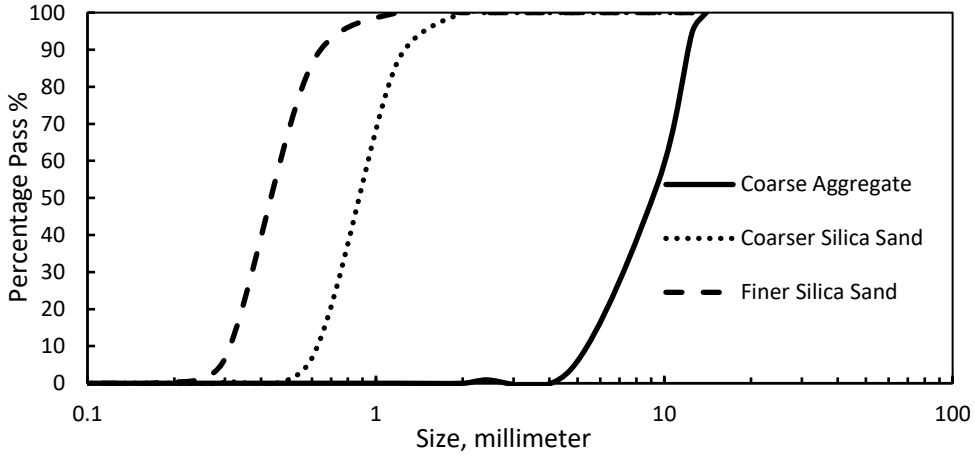

Figure 3.3. Particle size distributions of coarse and fine aggregates.

Table 3.1. The base UHPC mix design.

Material	Quantity, kg/m^3
Coarse aggregate	612
Coarser silica sand	500
Finer silica sand	500
Cement	604
Silica fume	268
Slag powder	120
Limestone powder	216
Water	144
Superplasticizer	57.6
Steel fiber	148

Ultra-high-performance concrete mixtures were prepared in the following steps using a rotary drum mixer:

1. Add all aggregates and powders to the mixer in the following sequence: coarse aggregate, fine aggregates, and powders (cement, silica fume, slag and limestone powder).
2. Dry-mix for two minutes.
3. Add water with half of the superplasticizer over two minutes, and mix for an additional half a minute.
4. Add the rest of the superplasticizer to the mix over one minute.
5. Continue mixing until a wet paste forms (usually 4 to 9 minutes).
6. Add the steel fibers to the mix.
7. Mix until a total mixing duration of 15 minutes is reached.
8. Cast the fresh UHPC mix into molds, and consolidate on a vibrating table over 5 minutes to minimize the entrapped air voids.

Materials and Methods for Resolving the UHPC Surface Issues

The materials and methods used together with the based UHPC mixtures for resolving the surface issues (elephant skin formation) are described in the following. MasterKure® ER50 (supplied by BASF) was used as an example evaporation reducer which, upon spraying on the fresh concrete surface, forms a film to reduce evaporation of water from the surface. Polypropylene fibers of 0.3 micrometer diameter and 12 mm length, supplied by Hoehn Plastics Incorporated, were used at 0.1% by weight of all solid materials to control surface plastic shrinkage cracking. Carbon fibers of 7.2 micrometer diameter and 13 mm length, supplied by Zoltek, were used at 0.1% by weight of all solid materials to control surface plastic shrinkage cracking. An acrylic latex (Latex R, supplied by Sika Corporation) was used at 0.1% by volume of all solid materials to internally form a film near the concrete surface in order to mitigate moisture loss and also achieve enhanced ductility and crack resistance. Cellulose ether (with viscosity of 10 MPa·s supplied by Dow Construction Chemicals), a water-soluble polymer derived from cellulose, was used to render film-forming and water-retention effects. A plastic sheet was used to cover the UHPC surface immediately after placement and finishing in order to reduce moisture loss.

The test procedures employed for evaluating the extent of elephant skin formation are described below.

A concrete slab of 35cmx35cm planar dimensions with 15cm thickness was prepared with the fresh UHPC mixture. The surface was troweled immediately after casting and consolidation. The slab was then placed in the test environment that is schematically depicted in Figure 3.4. This environment exposed the top surface of slab to 120Volts, 1000W, 60 Hz worklight, provided by SMART Electrician, with a fan producing a wind speed of 4.8m/s at a relative humidity of 58% The surface temperature of UHPC was recorded every 5 minutes during the test.

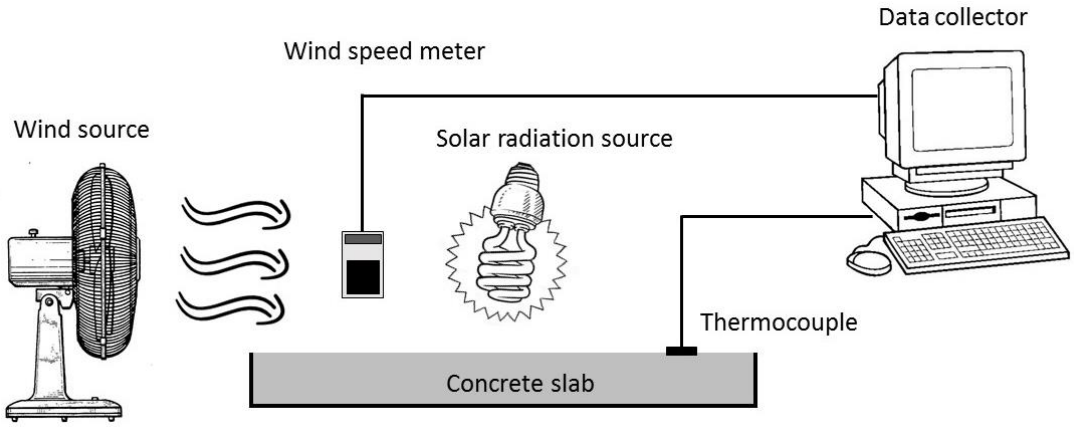

Figure 3.4. The test setup used to simulate elephant skin formation on the UHPC surface in field.

Penetrometer Test Method

The penetrometer test, used commonly for measurement of the concrete set time (ASTM C403), was employed in this investigation to measure the penetration resistance ('hardness') of the hardened skin formed on the exposed surface. Of UHPC This test was also performed on the bottom surface of UHPC (by turning the specimen upside down). Figure 3.5a shows the penetrometer test apparatus. The probe used for measurement of penetration resistance (Figure 3.5b) had a diameter of 9 mm and a length of 30 mm. Penetration tests were performed 140 minutes after addition of water to the mix.

Figure 3.5. The penetration test apparatus and test probe.

Test Results and Discussion

Figure 3.6 shows the visual appearance of the base UHPC surface; elephant skin formation and surface cracking were noted 10 minutes after exposure to the combination of air flow and radiation. A hard surface layer of about 3 cm thickness formed after about 50 minutes; the body of UHPC underneath this layer was soft at this time. These are characteristic features of elephant skin formation in conventional UHPC mixtures.

Figure 3.6. Surface appearance of the base UHPC mix, depicting elephant skin formation on the exposed surface.

Figure 3.7 presents the penetration test results for the top (exposed) and bottom surfaces of the slab made with the base UHPC mixtures versus time (starting at 140 minutes after addition of water to the mix). Hardening of the exposed surface is apparent is this figure. The exposed (top) surface has a penetration resistance that is about twice that of the bottom surface at 140 minutes after addition of water. The rate of hardening of the top surface continues to be higher than that of the bottom surface beyond this time; At 290 minutes after mixing, the penetration resistance of the top surface is about 4 times that of the bottom surface. These findings provide support for the hypothesis that loss of surface moisture from UHPC which has limited moisture content is a factor in elephant skin formation. The surface hardening associated with this moisture loss and its plastic shrinkage are expected to make key contributions to elephant skin formation.

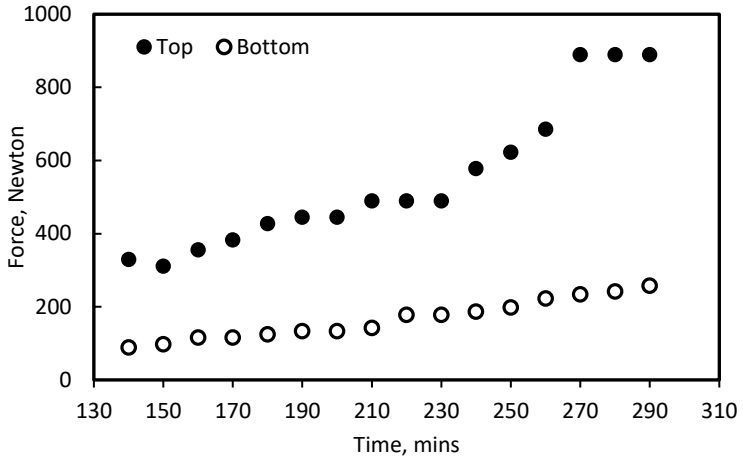

Figure 3.7. Measured values of penetration resistance versus time at the exposed (top) and bottom surfaces of the slab made with the base UHPC mix design.

Figure 3.8 shows the surface appearance of the UHPC mix modified with carbon fibers. The addition of carbon fibers produced a shiny surface, but was not highly effective in preventing the formation of elephant skin. Surface (plastic shrinkage) cracking formed after 40 minutes of exposure to air flow and radiation. A hard surface layer of about 4cm thickness also started forming after 45 minutes. A notable surface drying started after 47 minutes at corners, spreading gradually towards the center of the slab surface. Efforts were made to penetrate the surface with steel rods (Figure 3.9). While the surface layer was hard to penetrate, the concrete below this hardened layer remained soft. In short, carbon fibers could not effectively mitigate the major manifestations of elephant skin formation. They are probably ineffective in reducing moisture evaporation; they also did not exhibit desired plastic shrinkage crack control qualities in UHPC. The temperature difference between top and bottom layers was relatively small (few degrees centigrade); the surface temperature was actually higher due to the radiation effects. Water evaporation from the surface is probably the key factor governing elephant skin formation. It is worth mentioning that temperature rise at the concrete surface increases the rate of evaporation.

Figure 3.8. Surface appearance of the UHPC mix incorporating carbon fibers during the test.

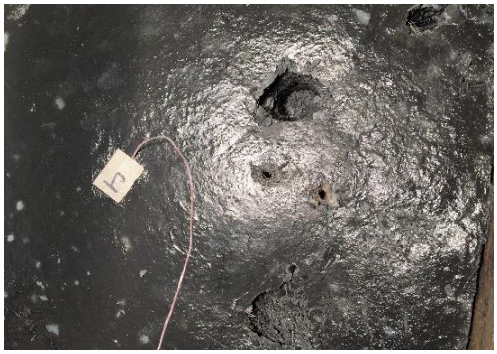

Figure 3.9. Surface appearance after attempts to penetrate the hardened surface layer with a steel rod after 1 hour of exposure to air flow and radiation.

The surface layer of the UHPC mix incorporating 0.1 vol.% of acrylic latex is shown in Figure 3.10 under air flow and radiation. Latex improved the fresh mix workability, and was effective in reducing elephant skin formation. The surface started to dry about 20 minutes after addition of the second batch of water during mixing. After 45 minutes, formation of a hard layer on the surface was noted; this layer, however, was only 1.5cm thick, that is half that formed on the based UHPC surface. The surface hardness (versus that of the bulk UHPC underneath the surface) was also less than that of the base UHPC mix.

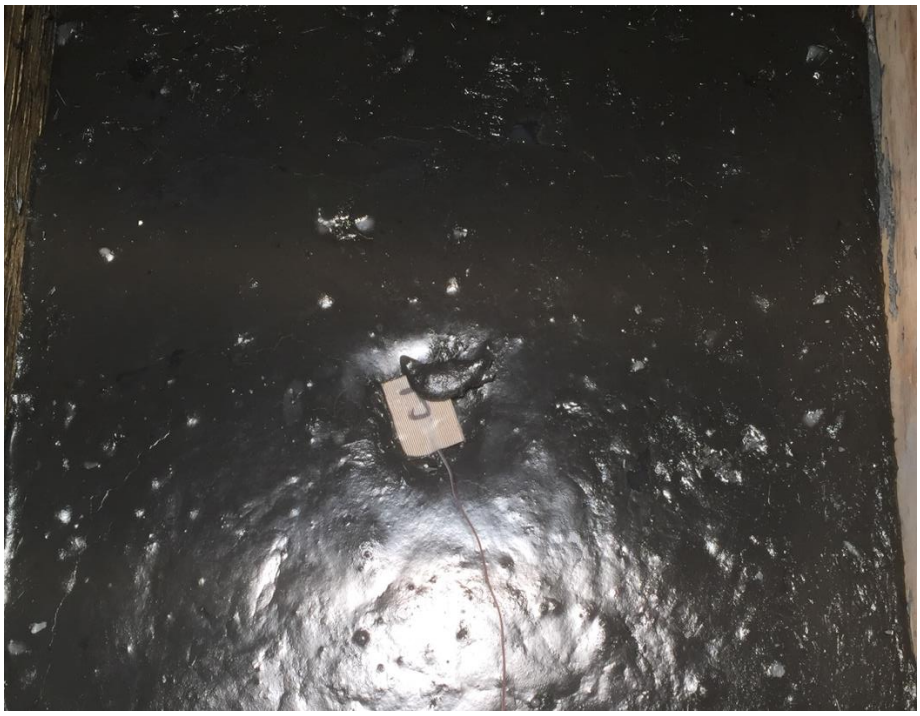

Figure 3.10. Surface appearance of the UHPC mix incorporating acrylic latex under air flow and radiation.

Figure 3.11 shows the penetration test results for the top (exposed) and bottom surfaces of the slab made with the latex modified UHPC mixture. When compared with the based UHPC mixture (Figure 3.7), introduction of latex at a relatively small dosage significantly lowered the penetration resistance of the top (exposed) surface layer, reducing the difference in the penetration resistance of top and bottom surfaces over time. This provides further indications of the value of (acrylic) latex in control of elephant skin formation. It should be noted the latex polymer was used in this application at 0.1 vol.%, which is very low when compared with the dosages of latex commonly used in concrete for enhancement of barrier qualities and other engineering properties. The cost implications of using latex for control of elephant skin formation on the exposed UHPC surfaces is thus minor.

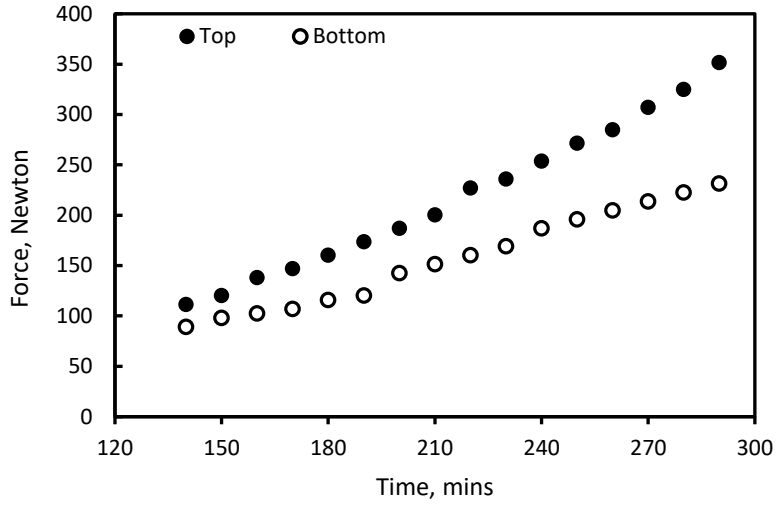

Figure 3.11. Measured values of penetration resistance versus time at the exposed (top) and bottom surfaces of the slab made with UHPC incorporating latex.

Figure 3.12 presents the penetration resistance versus time test results for the top and bottom surfaces of the slab prepared with the UHPC incorporating polypropylene fibers. When compared with the base UHPC mix (see Figure 3.7), Introduction of polypropylene fibers did not reduce the penetration resistance of top surface. The thickness of the hardened top layer was similar without and with polypropylene fibers. Figures 3.13a and 3.13b show the surface appearances of the polypropylene fiber reinforced UHPC slab prior to and after exposure to air flow and radiation. The presence of polypropylene fibers reduced the roughening effect of elephant skin formation on the exposed (top) surface, but cracks could still be observed on the top surface after exposure to air flow and radiation. Temperature measurements of the top and bottom surfaces of UHPC slabs reinforced with polypropylene fibers did not point at any noticeable effects of polypropylene fibers on trends in temperature rise with time.

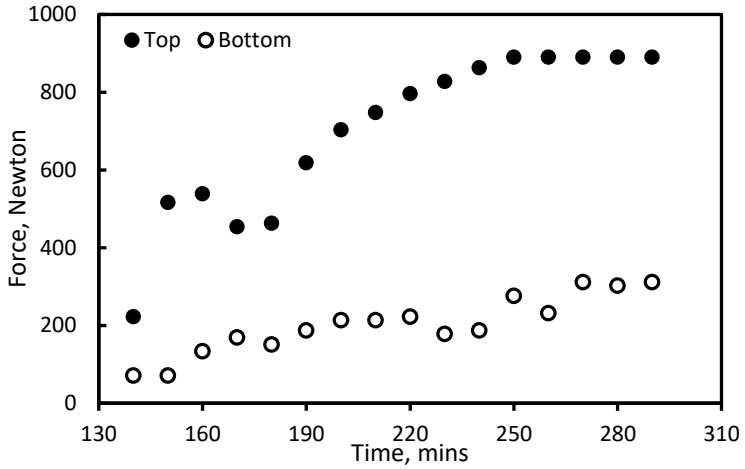

Figure 3.12. Measured values of penetration resistance versus time at the exposed (top) and bottom surfaces of the slab made with the addition of polypropylene.

Figure 3.13. Surface appearances of the UHPC mix incorporating polypropylene fibers prior to and after exposure to air flow and radiation.

Figure 3.14 and 3.15 present the penetration resistant test results versus time for UHPC slab sprayed with water and evaporation retarder, respectively. The slap top (exposed) surface was sprayed soon after placement and finishing of UHPC. When compared with the base (non-sprayed) UHPC slab (see Figure 3.7) spraying with water or evaporation retarder did not have significant effects on the rise in surface hardness. The thickness of the hardened (top) surface layer also did not change significantly with spraying of water or evaporation retarder solution. Elephant skin formation was also noted after exposure to air flow and radiation on top surfaces of UHPC slabs

sprayed with water or evaporation retarder (Figure 3.16). The trends in temperature rise with time of exposure to radiation and air flow were not changed with spray application.

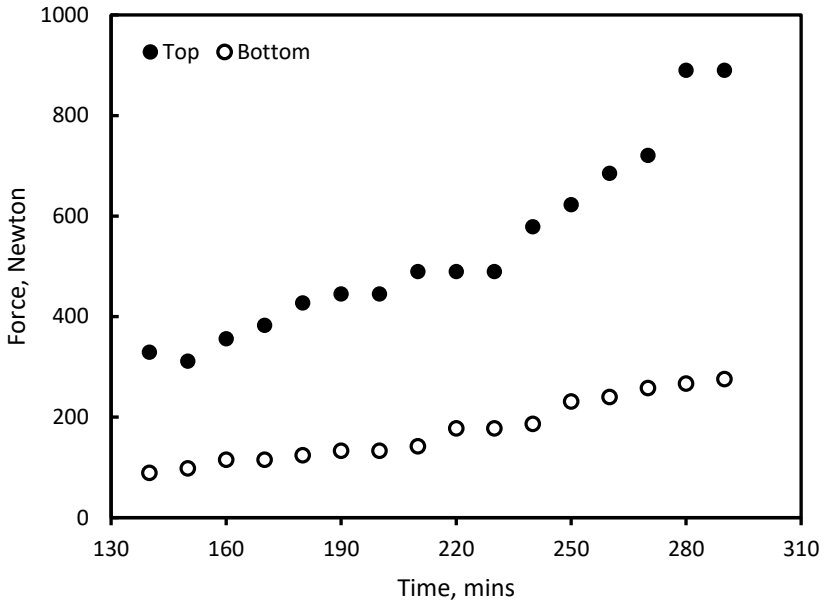

Figure 3.14. Measured values of penetration resistance versus time at the exposed (top) and bottom surfaces of the slab made with the base UHPC mix design with the spray of water.

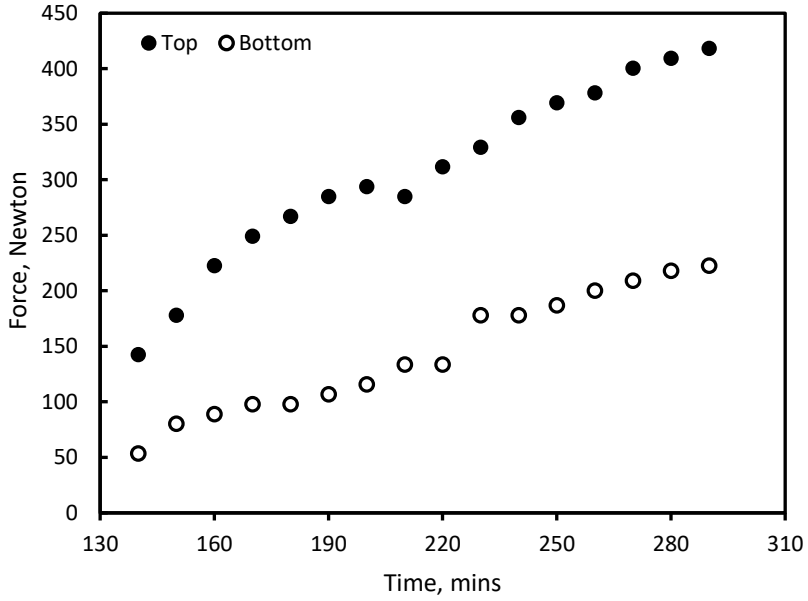

Figure 3.15. Measured values of penetration resistance versus time at the exposed (top) and bottom surfaces of the slab made with the base UHPC mix design with the spray of evaporation retarder.

(a)

(b)

Figure 3.16. Surface appearance of the UHPC mix sprayed with water (left) and evaporation retarder (right) prior to and after exposure to radiation and air flow (a) prior to exposure (b) after exposure.

Addition of cellulose ether to the UHPC mix was found to be ineffective in reducing surface hardening (Figure 3.17) and elephant skin formation on the exposed surface (Figure 3.18). The thickness of the hardened surface layer actually increased with 3cm (for the base UHPC mix) to 3.5cm for the UHPC mix incorporating cellulose ether. The trends in temperature rise with time of exposure to radiation and air flow also did not change significantly with introduction of cellulose ether into the UHPC mix.

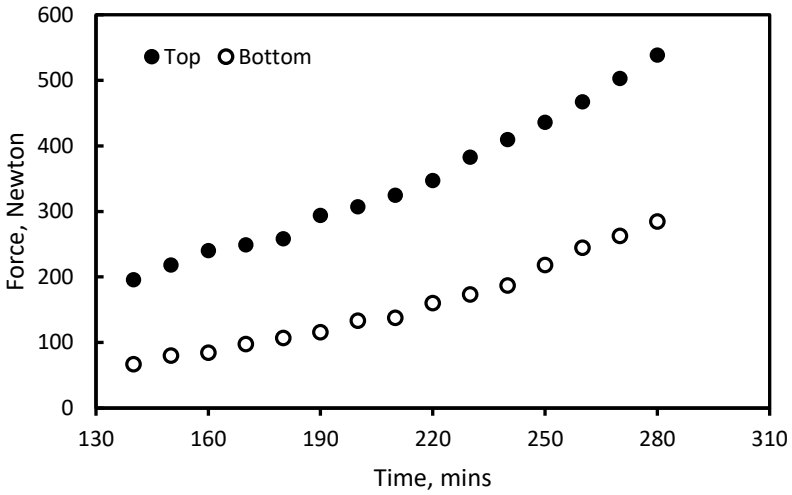

Figure 3.17. Measured values of penetration resistance versus time at the exposed (top) and bottom surfaces of the slab made with the UHPC mix incorporating cellulose ether.

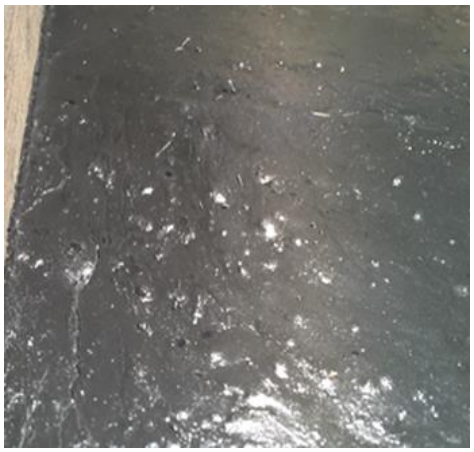

Figure 3.18. Surface appearance of the UHPC mix incorporating cellulose ether after exposure to air flow and radiation.

The above test results indicated that addition of latex polymer to the UHPC mix is the only effective means of controlling elephant skin formation on the exposed surfaces of UHPC. An attempt was also made to evaluate the effects of plastic sheet covering (Figure 3.21) for reducing the loss of moisture from the exposed surface of the UHPC slab under exposure to radiation and air flow. Covering with plastic sheet was found to be effective in reducing the trends towards hardening of the base UHPC mix under exposure to radiation and air flow (Figure 3.19).

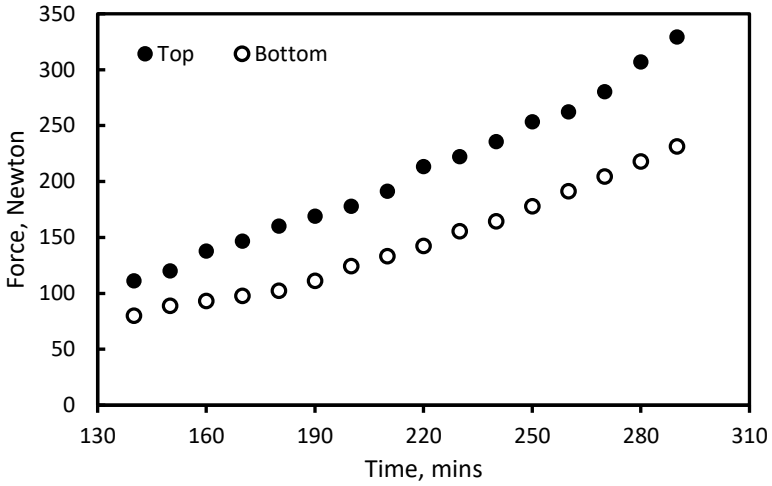

Figure 3.19. Measured values of penetration resistance versus time of exposure to radiation and flow for the slab made with the base UHPC mix which was covered with plastic sheet during exposure to radiation and air flow.

The penetration test results presented in Figure 3.20 as well as the surface appearance of the slab after exposure to radiation and air flow (Figure 3.22) indicate that the combination of the two effective measures did not produce significant improvements over the cases with each method implemented separately. It seems that both latex modification and plastic sheet coverage mitigate elephant skin formation by reducing moisture loss from the surface. It is, however, surprising that spraying the surface with water or an evaporation retarding solution was not found to be effective in reducing elephant skin formation.

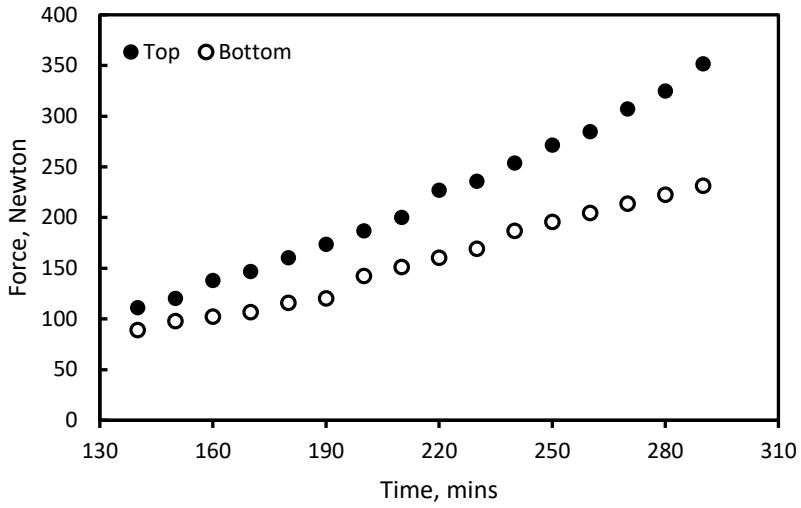

Figure 3.20. Measured values of penetration resistance versus time of exposure to radiation and flow for the slab made with the latex modified UHPC which was covered with plastic sheet during exposure to radiation and air flow.

Figure 3.21. Visual appearance of the slab covered with plastic sheet after exposure and air flow.

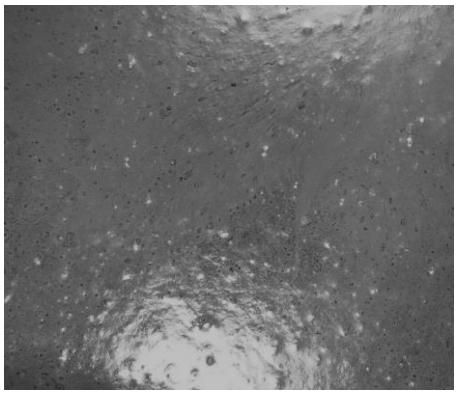

Figure 3.22. Visual appearance of the slab made with the latex modified UHPC mix and covered with plastic sheet after exposure to radiation and air flow.

Table 3.2 presents the measured values of the total crack area formed on the exposed (top) surfaces of UHPC slabs after exposure to radiation and air flow. Covering with plastic sheet eliminated formation of any visible cracks. Latex was the second effective measure against cracking which occurs with elephant skin formation. There is thus a correlation between the effectiveness of different measures in controlling elephant skin formation and preventing early-age cracking.

Table 3.2. Measured values of surface crack area after exposure to radiation and air flow.

	Base	Carbon Fiber	Polyprop Fiber	Evaporation Retarder	Water Spray	Cellulose Ether	Plastic Sheet Covering	Latex
surface crack area, cm^2	892.5	787.5	577.5	472.5	819	682.5	22.8	420

While plastic coverage of surface is a practice to be implemented during construction, latex modification is a change in material design which could affect the UHPC compressive strength. Therefore, compressive strengths of UHPC were assessed without and with latex modification. The UHPC mixtures were prepared as described earlier, and molded into 50mm cubic specimens using external vibration for consolidation. The specimens were demolded after 24 hours of storage in sealed condition at room temperature, and were subjected to steam curing at 90^{o}C for 48 hours. They were then stored at 50% relative humidity and room temperature for 3 days, after which they were subjected to compression test (ASTM C 39). Eight specimens were prepared from each mix. The compressive strength test results presented in Table 3.3 indicate that latex modification (considering that a relatively low concentration of latex was used for the purpose of controlling elephant skin formation) did not significantly alter the compressive strength of UHPC.

Table 3.3. Effect of latex modification on the compressive strength of UHPC (mean values and 95% confidence intervals).

	UHPC Base mix	UHPC with latex
Compressive strength, MPa	218.2 ±4.5	214.4 ±6.1

Conclusion

The combination of low moisture content, limited bleeding and high barrier qualities of ultra-high-performance concrete (UHPC) can lead to the formation of a rough texture with cracks on the exposed surfaces of UHPC. This phenomenon, occasionally referred to as 'elephant skin' formation occurs within few hours after placement of UHPC and finishing of its surface. Various strategies were evaluated for control of elephant skin formation on the exposed UHPC surfaces. These strategies emphasized reduction of moisture evaporation (application of curing membrane, covering with plastic sheet, low-concentration latex polymer modification, and use of cellulose ether as additive), enhancement of crack resistance in fresh state (synthetic fiber reinforcement and latex modification), and enhancement of dimensional stability (use of shrinkage reducing admixture or cellulose ether). The potential for elephant skin formation was assessed by subjecting the exposed surface of UHPC slab to a combination of air flow and radiation. Measurements were made on the surface penetration resistance and the temperature profile across the depth over time of exposure. After two hours of exposure to radiation and air flow, the visual appearance of the surface was judged, and the total surface crack area was measured. The conclusions derived in this experimental work are summarized below.

1. Latex modification and surface coverage with a plastic sheet immediately after finishing are the most effective measures against elephant skin formation. These measures helped

with retaining the surface aesthetics and controlled surface cracking. Lower values of surface penetration resistance were obtained with these measures, which points at the value of penetration resistance as an indicator of elephant skin formation. The combination of latex polymer modification and plastic sheet covering did not bring about improvements, when compared with plastic sheet covering alone. In addition, latex polymer modification did not compromise the UHPC compressive strength. The use of latex at a relatively low concentration in this application minimizes its cost implications.

2. Use of synthetic fibers, shrinkage-reducing admixture, cellulose ether and curing membrane did not lead to effective control of elephant skin formation. Visual observations as well as measurements of surface penetration resistance and crack area confirmed formation of elephant skin in spite of implementing these measures.

3. The findings of this experimental study indicate that evaporation of surface moisture (which is accompanied by self-desiccation), considering the low moisture content of UHPC, is probably the primary cause of elephant skin formation. Plastic sheet covering of the exposed surface and latex modification of UHPC probably control elephant skin formation through reduction of moisture loss form the exposed surface. Measures such as synthetic fiber reinforcement and use of shrinkage reducing admixtures, which enhance the resistance of concrete to plastic shrinkage cracking without reducing moisture loss, do not reduce elephant skin formation. This finding points at the distinctions between plastic shrinkage cracking of concrete and elephant skin formation on ultra-high-performance concrete.

CHAPTER 4

Experimental Investigations of the Dimensional Stability and Durability of Ultra-High-Performance Concrete

Abstract

An experimental investigation was conducted in order to provide further insight into the material properties of UHPC. The aspects of UHPC performance investigated in this work included dimensional and chemical stability, sorption resistance, and freeze-thaw durability. UHPC was found to produce a desired balance of dimensional and chemical stability, and distinctly low sorptivity and water absorption capacity. The heat of hydration of UHPC was also relatively low. UHPC, unlike a normal Portland cement paste exhibited autogenous shrinkage; the amount of this shrinkage was, however, relatively small. These test results were explained based on the distinctly low water content, the high pozzolan content of the cementitious binder in UHPC, and the high dosage of superplasticizer used in UHPC mixtures. The fact that water content of UHPC is not adequate for thorough hydration of cementitious particles seems to be a significant factor influencing those aspects of the UHPC behavior evaluated in this investigation.

Introduction

Ultra-high-performance Concrete(UHPC) refers to cement-based materials with compressive strengths exceeding 150 MPa, with also provide high ductility and excellent durability (Shi et al., 2015). UHPC materials are also expected to provide desired flowability for reliable construction at high speed (Schießl et al., 2007). UHPC was first introduced in the mid-1990s, with heat curing, extensive vibration and longer mixing times (Richard and Cheyrezy, 1995). The high cementitious paste content, the fine pore system, and the potential for chemical/autogenous shrinkage tend to compromise the dimensional stability of UHPC, which would otherwise benefit from a low

water/cement ratio (Holt, 2005, Zhang et al., 2003, Tazawa et al., 1995, Lura et al., 2003, Barcelo et al., 2005, mejlhede Jensen and Freiesleben Hansen, 1996).

The high resistance of UHPC against transport of moisture and dissolved chemicals is an important aspect of its behavior. Restrained shrinkage cracking of UHPC can undermine this highly desired quality. As far as shrinkage cracking is prevented, UHPC is knows to provide highly desirable durability characteristics under adverse exposure conditions (Pierard et al., 2012, Acker and Behloul, 2004). Hence, besides improvements in structural efficiency, UHPC applications can lead to a significant rise in the service life of the concrete-based infrastructure. For UHPC, sufficient curing is essential for a concrete to provide its potential performance (Khatri et al., 1997, Hooton et al., 1993). The durability of concrete subjected to aggressive environments depends largely on transport properties, which are influenced by pore system (Sabir et al., 1998, Glasser et al., 2008, Pipilikaki and Beazi-Katsioti, 2009, Parrott, 1992, ASTM, 2004). Pozzolanic materials commonly used include fly ash, silica fume and metakaolin; these materials are usually added to concrete as constituent of blended cement or at the concrete batch plant as a partial replacement. Addition of these materials mostly can enhance various aspects of concrete durability.

Ultra-high-performance concrete provides a segmented capillary pore system which enhance its barrier and durability characteristics (Amanchukwu et al., 2015). The surface layer of UHPC, however, could be compromised by a combination of drying and autogenous shrinkage considering that the surface water cannot be replenished due to its low bleeding (Bentur et al., 2001, Zhu et al., 2016). Given the emphasis on high strength, air-entrainment is not commonly practice with UHPC. This approach assumes that the high barrier qualities of UHPC provide it with desired freeze-thaw durability (Papadakis et al., 1991).

Materials and Methods

Materials

The granular raw materials used in the UHPC mix design considered in this investigation can be divided into two categories: (1) cementitious materials and fine filler (limestone powder); and (2) aggregates. The cementitious materials and the fine filler considered in this investigation were: (i) Type I Portland cement; (ii) undensified silica fume with ~200 nm mean particle size, ~15 m^2/g specific area and >105% 7-day pozzolanic activity index; (iii) ground granulated blast furnace slag with specific gravity of 2.9 and bulk density of 1,200 kg/m^3, ground to less than 45 micrometer particle size; and (iv) limestone powder with 2 micrometer mean particle size. The particle size distributions of cementitious materials and limestone powder are presented in figure 4.1. The aggregates used in UHPC mixtures included (see Figure 4.2 for particle size distributions) (i) limestone coarse aggregate with 12 mm maximum size; (ii) coarse silica sand with mean particle size of 0.8 mm and specific gravity of 2.67; and (iii) fine silica sand with mean particle size of 0.4 mm and specific gravity of 2.65. A polycarboxylate-based superplasticizer (Chryso 150 supplied by Chryso, with 1.06 specific gravity and 1.8% solid content) and steel fiber of 0.2mm diameter and 15mm length with brass coating (supplied by Bekaert) were also used in UHPC mixtures. The UHPC mix design considered in this investigation is presented in Table 4.1.

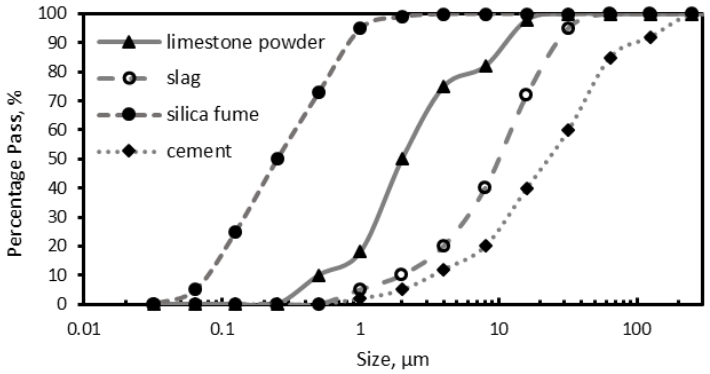

Figure 4.1. Particle size distribution of the cementitious materials and limestone powder.

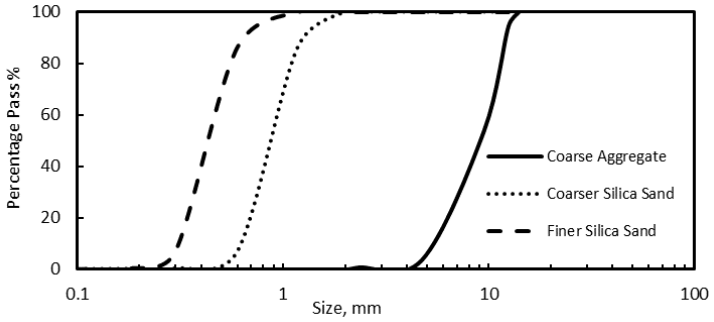

Figure 4.2. Particle size distribution of coarse and fine aggregates.

Table 4.1. UHPC mix design.

Material	Quantity, kg/m^3
Coarse aggregate	612
Coarser silica sand	500
Finer silica sand	500
Cement	604
Silica fume	268
Slag powder	120
Limestone powder	216
Water	144
Superplasticizer	57.6
Steel fiber	148

Methods

Ultra-high-performance concrete mixtures were prepared in the following steps using a rotary drum mixer:

1. Add all aggregates and powders to the mixer in the following sequence: coarse aggregate, fine aggregates, and powders (cement, silica fume, slag and limestone powder).

2. Dry-mix for two minutes.
3. Add water with half of the superplasticizer over two minutes, and mix for an additional half a minute.
4. Add the rest of the superplasticizer to the mix over one minute.
5. Continue mixing until a wet paste forms (usually 4 to 9 minutes).
6. Add the steel fibers to the mix.
7. Mix until a total mixing duration of 15 minutes is reached.

The resulting fresh concrete mixtures were cast in molds and consolidated using a vibrating table. The molded specimens were stored under sealed condition, and demolded after 24 hours. Unless specified otherwise for specific tests in the following description, the specimens were subjected to steam curing at 90^{o}C for 48 hours. The specimens were then stored at 50% relative humidity and room temperature for 3 days.

Drying shrinkage tests were performed following the ASTM C596 procedures. Mortar mixture was prepared using the same materials presented in Table 4.1 (without coarse aggregate). The mortar specimens were cast on 25mmx25mmx285mm steel moles. Following the ASTM C157 requirements, the specimens were moist-cured inside molds for 24 h ± 30 minutes. They were then cured in lime-saturated water for 72 h ± 30 minutes, when the initial length was recorded.

Figure 4.3. Drying shrinkage set up.

Autogenous shrinkage experiments were performed per ASTM C 1698. A corrugated plastic tube of 30 mm diameter and 420 mm length was capped and sealed at one end, and was filled with UHPC while held vertically. The open end was then capped and sealed. The filled corrugated tubes were kept in a length measurement instrument (Figure 4.4) at 50% relative humidity and 22^{o}C, with an LVDT contacting the specimen end (with the other end fixed) to measure length change as a function of time. While ASTM C1698 starts length measurements after final set, the length measurements in this study were initiated immediately after mixing and placement in corrugated tubes. For comparison purposes, similar tests were also performed with Portland cement. It is worth mentioning that the initiation of length measurement immediately after placement of fresh mix in tube is not uncommon (Blandine et al., 2016).

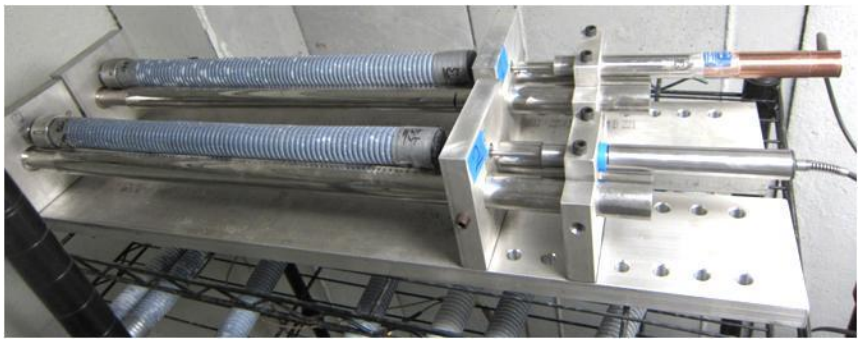

Figure 4.4. The autogenous shrinkage test setup.

Sorptivity tests were conducted per ASTM C1585, using 10 cm x 5 cm cylindrical specimen. This test measures the rate of capillary sorption of cured specimens after conditioning their moisture content to a standard level.

Autoclave expansion tests were performed per ASTM C151. This test was performed on the UHPC paste specimens prepared by mixing the (micro- and nano-scale) powder constituents of UHPC with water and superplasticizer to produce a paste of normal consistency.

The heat of hydration for the UHPC paste was measured per ASTM C1679. This test was also performed on the UHPC paste prepared by mixing the powder constituents of UHPC with water and superplasticizer to produce a paste of normal consistency.

The freeze-thaw experiments were performed per ASTM C666, with both freezing and thawing occurring in water. The freeze-thaw test setup is shown in Figure 4.5. The effects of freeze-thaw cycles on the dynamic modulus of elasticity and weight of UHPC specimens were investigated.

Figure 4.5. Freeze-thaw test chamber.

Results and Discussion

Drying Shrinkage

The drying shrinkage test results are presented in Figure 6 for UHPC, together with typical data for normal-strength concrete. UHPC is rich in cementitious paste content, with relatively high proportions of pozzolanic materials, which tend to increase its shrinkage movements. On the other hand, the very low water content of UHPC tends to lower its drying shrinkage. The comparison made with normal-strength concrete in Figure 6 indicates that the drying shrinkage of UHPC is comparable to that of normal-strength concrete. The low water content of UHPC can be used to explain this finding. This water content is below that required for hydration of the cementitious powder, therefore, cores of cementitious powders remain unhdrated; they act as well-bonded dense fillers within cement hydrates, which restrain their shrinkage movements.

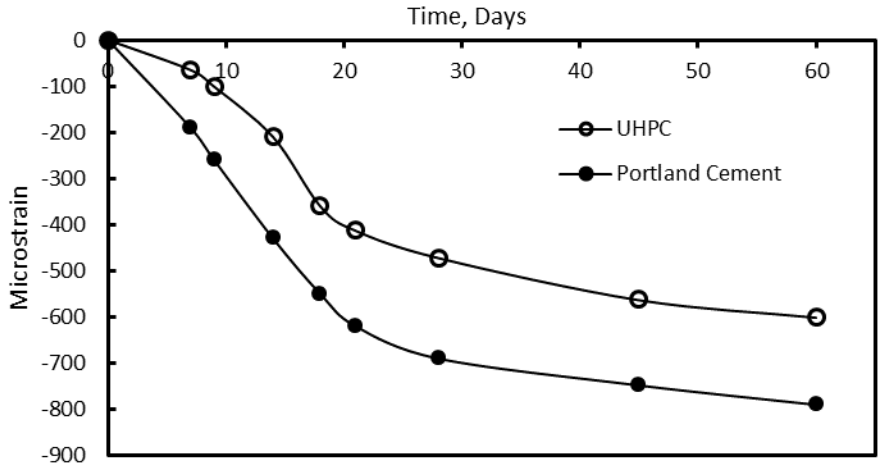

Figure 4.6. Drying shrinkage test results.

Autogenous shrinkage

The autogenous shrinkage test results for the UHPC mortar and a Type I Portland cement mortar are presented in Figures 4.7a and 4.7b, respectively. The overall shrinkage of the UHPC is

observed to be smaller than that of Portland cement mortar. In both cases a rapid rate of shrinkage is observed initially. This rapid shrinkage takes place over about 15 and 2 hours in the case of the UHPC and Portland cement mortars, respectively. These are movements which seem to occur until the paste reaches a certain level of setting. The presence of high superplasticizer contents and pozzolans in the UHPC mortar delay its set time, which could explain why the initial rapid rate of shrinkage occurs over an extended time period. While the overall shrinkage movements of the UHPC mortar are lower than those of Portland cement paste, the autogenous shrinkage movements of the UHPC mortar continue to occur over time (up to 200 hours considered here). In the case of Portland cement mortar, however, shrinkage movements stop after the initial period of 2 hours. One can argue that these long-term movements are the primary ones caused by autogenous shrinkage. This would imply that autogenous shrinkage (after the initial period of rapid shrinkage) cannot be detected in the case of Portland cement mortar, but is detectable for the UHPC mortar.

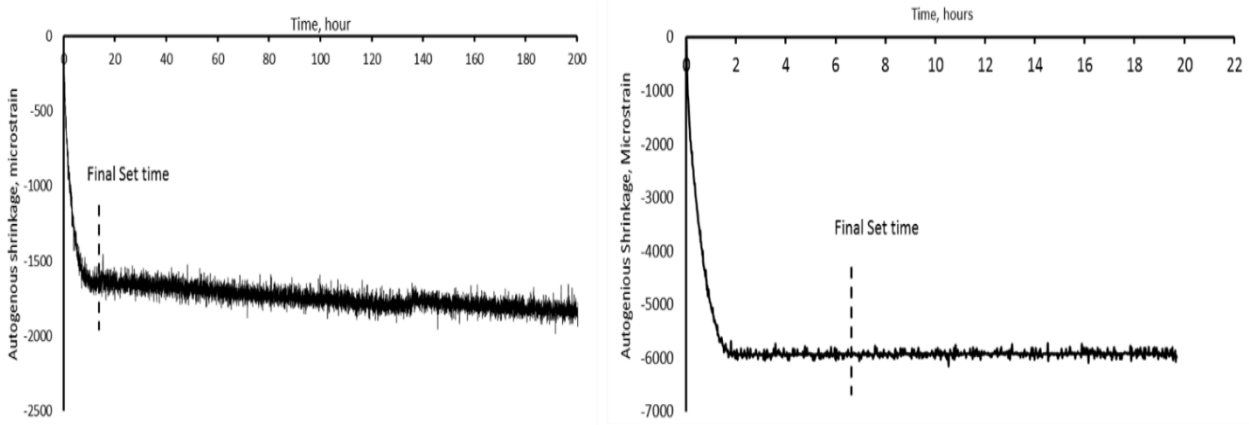

(a) UHPC paste (b) Portland cement paste

Figure 4.7. Autogenous shrinkage test results.

Heat of hydration

The heat of hydration test results for UHPC are presented in Figure 4.8a; typical data for Type I Portland cement are presented in Figure 4.8b. The rates of heat release of the UHPC cementitious

paste are observed to be well below those of Portland cement. The dormant period with UHPC is also longer than that for Portland cement. These findings can be explained by: (i) the very low water content of the UHPC paste, enabled by the use of a high dosage of superplasticizer, which is not adequate to fully hydrate the cementitious materials; (ii) the relatively high dosage of pozzolans among the cementitious materials of the UHPC paste; and (iii) probable retarding effects.

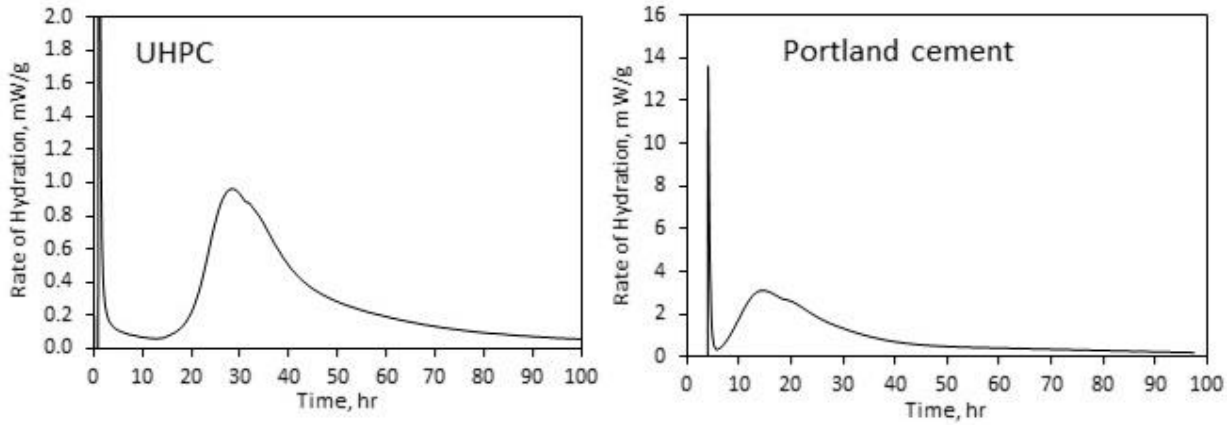

(a) UHPC (b) Typical Type I Portland Cement

Figure 4.8. Heat of Hydration tests results for UHPC and Portland cement.

Sorptivity

The sorptivity test results for UHPC and normal-strength concrete are presented in Figure 9. The initial and secondary sorption rates of UHPC are 0.20 and 0.10 $\mu m/s^{1/2}$, respectively, compared to 5.6 and 0.7 $\mu m/s^{1/2}$, respectively for normal-strength concrete (Table 4.2). The very low water content of UHPC significantly reduces its capillary porosity and thus capillary sorption capacity.

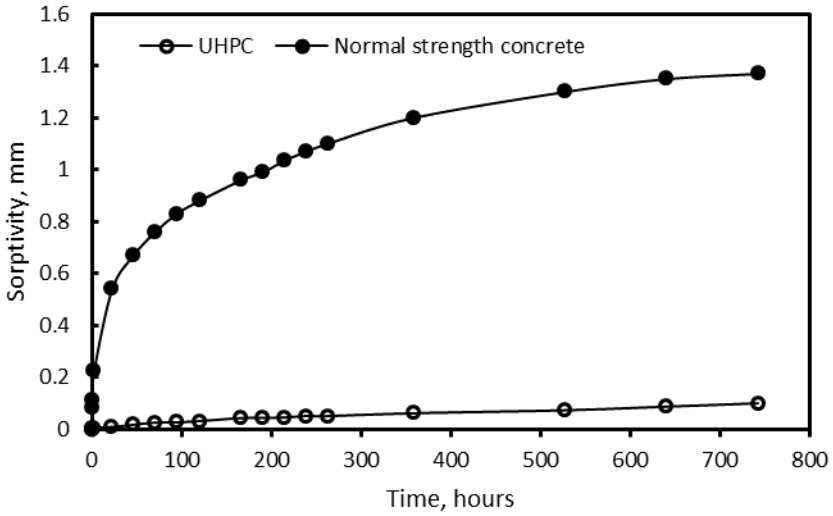

Figure 4.9. Sorptivity test results.

Table 4.2. Initial and secondary sorptivity values.

	Initial Sorptivity, $\mu m/s^{1/2}$	Secondary, $\mu m/s^{1/2}$
Normal strength concrete	5.60	0.70
UHPC	0.20	0.10

Autoclave Expansion

Autoclave expansion is an accelerated soundness tests that was used to evaluate the chemical stability of UHPC. The autoclave expansion tests results generated in this work for UHPC and normal-strength concrete are presented in Table 4.3. The autoclave expansion of UHPC (0.162%) is less than that of normal-strength concrete (0.38%) and well below the maximum limit of 0.8% required by ASTM C1157. Given the hydration mechanisms of the UHPC paste, one expects that the elevated temperature of autoclave raise the extent (and rate) of hydration in the case of UHPC, thus benefiting the end product structure and properties.

Table 4.3. Autoclave Expansion Results.

	Autoclave length change, %
Normal strength concrete	0.38 ± 0.02
UHPC	0.162±0.01

Freezing and Thawing

The measured values of dynamic modulus, expressed as percentage of unaged values, are presented in Figure 4.10 versus the number of applied freeze-thaw cycles. The corresponding weight loss test data are presented in Figure 4.11. Both these test results point at the high degree of freeze-thaw durability provided by UHPC. This is in spite of the fact that UHPC was subjected to freeze-thaw cycles without any air entrainment. The relatively low moisture content of UHPC lowers the damaging effects of freeze-thaw cycles.

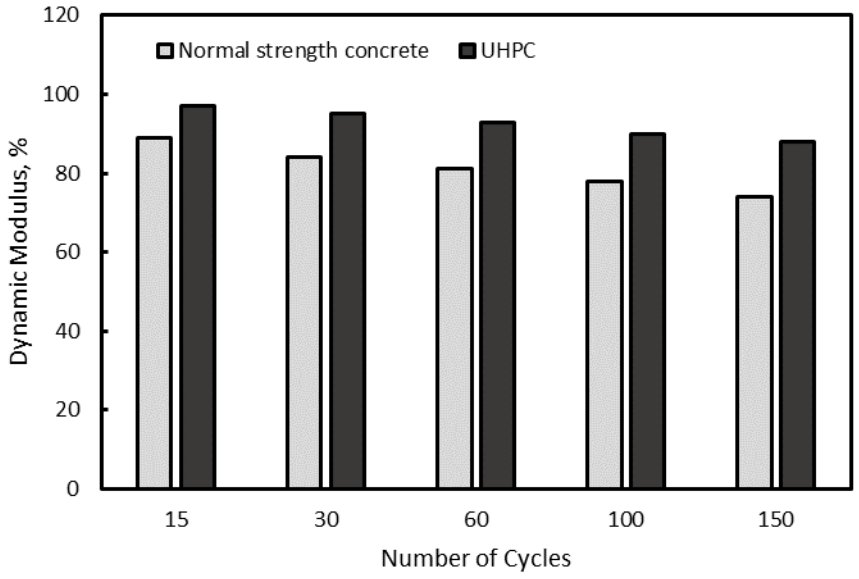

Figure 4.10. Dynamic modulus.

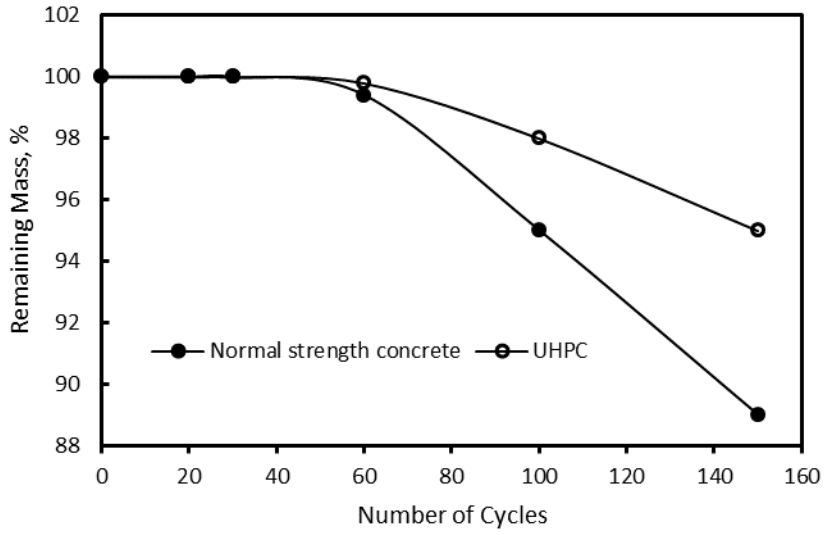

Figure 4.11. Remaining mass after freeze thaw cycle.

Conclusion

Investigations of the dimensional and chemical stability, heat of hydration, barrier qualities and durability characteristics of UHPC in this project yielded the following conclusions.

1. The very low water content of UHPC significantly lowered its capillary porosity and thus capillary sorptivity and water absorption capacity. This feature provides UHPC with distinct barrier qualities which significantly benefit its durability characteristics.
2. The heat of hydration of the UHPC paste was found to be relatively small in spite of its very high content of cementitious materials. This observation was attributed to: (i) the very low water content of the UHPC paste, which incorporates a high dosage of superplasticizer, that is not adequate to fully hydrate the cementitious materials; (ii) the relatively high dosage of pozzolans among the cementitious materials of the UHPC paste; and (iii) the probable retarding effect of the high superplasticizer content of this paste.

3. The presence of high superplasticizer contents and pozzolans in the UHPC paste delay its set time. The hydration process thus occurs over extended time periods; This observation together with the high moisture barrier qualities of UHPC can be used to explain the extended period during which the UHPC paste undergoes shrinkage movements. The drying shrinkage movements of UHPC were significantly below that of a Portland cement paste. This was in spite of the high cementitious materials content of the UHPC paste, and can be attributed to the very low water content of UHPC which leaves a notable fraction of the cementitious particles non-hydrated at their cores. These non-hydrated cores could act as fillers that actually reduce the UHPC paste drying shrinkage movements.
4. UHPC exhibits autogenous shrinkage movements over extended time periods. This is expected because the water in pore solution used in hydration of cementitious materials causes drying of these pores due to the limited water content of UHPC mixtures. The amount of UHPC autogenous shrinkage, however, is relatively small when compared with those caused by other sources of dimensional movement (e.g., drying shrinkage).
5. UHPC provided high levels of freeze-thaw durability without the need for air-entrainment. This was attributed to the low sorptivity and water absorption capacity of UHPC. The limited capillary porosity of UHPC significantly reduces the moisture content residing in these pores, thus reducing the damage caused by freeze-thaw cycles.

BIBLIOGRAPHY

BIBLIOGRAPHY

Adhikari, B., et al., *Stickiness in foods: a review of mechanisms and test methods.* International Journal of Food Properties, 2001. **4**(1): p. 1-33.

Aïtcin, P.-C., *High performance concrete*. 2011: CRC Press.

Aïtcin, P.-C., G. Haddad, and R. Morin, *Controlling Plastic and Autogenous Shrinkage in High-Performance Concrete Structures by an Early Water Curing.* Special Publication, 2004. **220**: p. 69-83.

Banfill, P., *Additivity effects in the rheology of fresh concrete containing water-reducing admixtures.* Construction and Building Materials, 2011. **25**(6): p. 2955-2960.

Barnett, S.J., et al., *Assessment of fibre orientation in ultra high performance fibre reinforced concrete and its effect on flexural strength.* Materials and Structures, 2010. **43**(7): p. 1009-1023.

Bentur, A., S.-i. Igarashi, and K. Kovler, *Prevention of autogenous shrinkage in high-strength concrete by internal curing using wet lightweight aggregates.* Cement and concrete research, 2001. **31**(11): p. 1587-1591.

Blais, P.Y. and M. Couture, *Precast, prestressed pedestrian bridge: World's first Reactive Powder Concrete structure.* PCI journal, 1999. **44**(5): p. 60-71.

Choi, M.S., et al., *Estimation of rheological properties of UHPC using mini slump test.* Construction and Building Materials, 2016. **106**: p. 632-639.

Choi, M., et al., *Lubrication layer properties during concrete pumping.* Cement and Concrete Research, 2013. **45**: p. 69-78.

Choi, M.S., Y.J. Kim, and S.H. Kwon, *Prediction on pipe flow of pumped concrete based on shear-induced particle migration.* Cement and Concrete Research, 2013. **52**: p. 216-224.

Cumberland, D. and R.J. Crawford, *The packing of particles.* 1987.

D Ambrosia, M., D. Lange, and Z. Grasley, *Measurement and modeling of concrete tensile creep and shrinkage at early age.* ACI SPECIAL PUBLICATIONS, 2004: p. 99-112.

Draijer, W., *Assessing the pumpability of concrete with the slump and pressure bleeding test: research on suitable test methods for assessing the pumpability of concrete.* 2007.

Elrahman, M.A. and B. Hillemeier, *Combined effect of fine fly ash and packing density on the properties of high performance concrete: An experimental approach.* Construction and Building Materials, 2014. **58**: p. 225-233

Ghafari, E., et al., *Prediction of Fresh and Hardened State Properties of UHPC: Comparative Study of Statistical Mixture Design and an Artificial Neural Network Model.* Journal of Materials in Civil Engineering, 2015. **27**(11): p. 04015017.

Graybeal, B., *Ultra-high performance concrete*. 2011

Habel, K., et al., *Development of the mechanical properties of an ultra-high performance fiber reinforced concrete (UHPFRC).* Cement and Concrete Research, 2006. **36**(7): p. 1362-1370.

Holt, E., *Contribution of mixture design to chemical and autogenous shrinkage of concrete at early ages.* Cement and concrete research, 2005. **35**(3): p. 464-472.

Hossain, K.M.A., *Volcanic ash and pumice as cement additives: pozzolanic, alkali-silica reaction and autoclave expansion characteristics.* Cement and Concrete Research, 2005. **35**(6): p. 1141-1144.

Jones, M., L. Zheng, and M. Newlands, *Estimation of the filler content required to minimise voids ratio in concrete.* Magazine of concrete research, 2003. **55**(2): p. 193.

Kang, S.-T. and J.-K. Kim, *The relation between fiber orientation and tensile behavior in an Ultra High Performance Fiber Reinforced Cementitious Composites (UHPFRCC).* Cement and Concrete Research, 2011. **41**(10): p. 1001-1014.

Kelham, S., *A water absorption test for concrete.* Magazine of Concrete Research, 1988. **40**(143): p. 106-110.

Kunieda, M. and K. Rokugo, *Recent progress on HPFRCC in Japan required performance and applications.* Journal of Advanced Concrete Technology, 2006. **4**(1): p. 19-33.

Kwan, A. and W. Fung, *Roles of water film thickness and SP dosage in rheology and cohesiveness of mortar.* Cement and Concrete Composites, 2012. **34**(2): p. 121-130.

Kwan, A., W. Fung, and H. Wong, *Water film thickness, flowability and rheology of cement-sand mortar.* Advances in Cement Research, 2010.

Lamond, J.F. and J.H. Pielert. *Significance of tests and properties of concrete and concrete-making materials*. 2006. ASTM West Conshohocken, PA

Lange, F., H. Mörtel, and V. Rudert, *Dense packing of cement pastes and resulting consequences on mortar properties.* Cement and concrete research, 1997. **27**(10): p. 1481-1488.

de Larrard, F. and T. Sedran, *Optimization of ultra-high-performance concrete by the use of a packing model.* Cement and Concrete Research, 1994. **24**(6): p. 997-1009.

Li, L. and A. Kwan, *Mortar design based on water film thickness.* Construction and Building Materials, 2011. **25**(5): p. 2381-2390.

Li, L.G. and A.K. Kwan, *Concrete mix design based on water film thickness and paste film thickness.* Cement and Concrete Composites, 2013. **39**: p. 33-42.

Li, P., et al., *Fresh behaviour of Ultra-high Performance Concrete (UHPC): an investigation of the effect of superplasticizers and steel fibres.* 2016.

Lowke, D., *Interparticle forces and rheology of cement based suspensions*, in *Nanotechnology in Construction 3*. 2009, Springer. p. 295-301.

Mays, G.C., *Durability of concrete structures: investigation, repair, protection*. 2002: CRC Press.

Peyvandi, A., et al., *Effect of the cementitious paste density on the performance efficiency of carbon nanofiber in concrete nanocomposite.* Construction and Building Materials, 2013. **48**: p. 265-269.

Pietsch, W., *Size enlargement by agglomeration*, in *Handbook of Powder Science & Technology*. 1997, Springer. p. 202-377.

Powers, T.C., *The properties of fresh concrete.* 1969

Richard, P. *Reactive powder concrete: a new ultra-high-strength cementitious material*. in *4th International Symposium on Utilization of High strength/High performance concrete, Paris*. 1996.

Richard, P. and M. Cheyrezy, *Composition of reactive powder concretes.* Cement and concrete research, 1995. **25**(7): p. 1501-1511.

Russell, H.G. and B.A. Graybeal, *Ultra-high performance concrete: A state-of-the-art report for the bridge community*. 2013.

Rüsch, H., D. Jungwirth, and H.K. Hilsdorf, *Creep and shrinkage: their effect on the behavior of concrete structures*. 2012: Springer Science & Business Media.

Sbia, L.A., et al., *Production methods for reliable construction of ultra-high-performance concrete (UHPC) structures.* Materials and Structures, 2017. **50**(1): p. 7.

Schießl, P., O. Mazanec, and D. Lowke, *SCC and UHPC—effect of mixing technology on fresh concrete properties*, in *Advances in Construction Materials 2007*. 2007, Springer. p. 513-522.

Schmidt, M., E. Fehling, and C. Geisenhanslüke. *Ultra high performance concrete (UHPC)*. in *Proceedings of the second international symposium on ultra high performance concrete, Kassel University Press, Germany*. 2004.

Schmidt, M. *Sustainable building with ultra-high-performance concrete (UHPC)—Coordinated research program in Germany*. in *Proceedings of Hipermat 2012 3rd International Symposium on UHPC and Nanotechnology for High Performance Construction Materials, Kassel University Press, Kassel*. 2012.

Scott, D.A., et al., *Impact of Steel Fiber Size and Shape on the Mechanical Properties of Ultra-High Performance Concrete*. 2015, DTIC Document.

Šerelis, E., V. Vaitkevičius, and V. Kerševičius, *Influence of silica fume on the workability and hydration process of ultra-high performance concrete.* Chemical Technology, 2016. **67**(1): p. 58-65.

Shen, S. and H. Yu, *Characterize packing of aggregate particles for paving materials: Particle size impact.* Construction and Building Materials, 2011. **25**(3): p. 1362-1368.

Shi, C., et al., *A review on ultra high performance concrete: Part I. Raw materials and mixture design.* Construction and Building Materials, 2015. **101**: p. 741-751.

Tazawa, E.-i., *Autogenous shrinkage of concrete*. 1999: CRC Press.

Uno, P.J., *Plastic shrinkage cracking and evaporation formulas.* ACI Materials Journal, 1998. **95**: p. 365-375.

Van Der Putten, J., K. Lesage, and G. De Schutter. *Influence of the Particle Shape on the Packing Density and Pumpability of UHPC*. in *Ultra-High Performance Concrete and High Performance Construction Materials (HIPERMAT)*. 2016.

Wong, H.H. and A.K. Kwan, *Packing density of cementitious materials: part 1—measurement using a wet packing method.* Materials and structures, 2008. **41**(4): p. 689-701.

Wu, Z., et al., *Effects of steel fiber content and shape on mechanical properties of ultra high performance concrete.* Construction and Building Materials, 2016. **103**: p. 8-14.

Yoo, D.-Y., H.-O. Shin, and Y.-S. Yoon, *Ultrasonic Monitoring of Setting and Strength Development of Ultra-High-Performance Concrete.* Materials, 2016. **9**(4): p. 294.

Yoo, D.-Y., S.-T. Kang, and Y.-S. Yoon, *Effect of fiber length and placement method on flexural behavior, tension-softening curve, and fiber distribution characteristics of UHPFRC.* Construction and Building Materials, 2014. **64**: p. 67-81

Yu, A., J. Bridgwater, and A. Burbidge, *On the modelling of the packing of fine particles.* Powder technology, 1997. **92**(3): p. 185-194.

Yu, R., P. Spiesz, and H. Brouwers, *Development of an eco-friendly Ultra-High Performance Concrete (UHPC) with efficient cement and mineral admixtures uses.* Cement and Concrete Composites, 2015. **55**: p. 383-394.

Zhang, M.-H., et al., *Measurement of yield stress for concentrated suspensions using a plate device.* Materials and Structures, 2010. **43**(1-2): p. 47-62.

Zhang, Q., et al., *Effect of Superplasticizers on Apparent Viscosity of Cement-Based Material with a Low Water–Binder Ratio.* Journal of Materials in Civil Engineering, 2016: p. 04016